

Concept of the Exhumed Partial Annealing (Retention) Zone and Age-Elevation Profiles in Thermochronology

Paul G. Fitzgerald and Marco G. Malusà

Abstract

Low-temperature thermochronology is commonly applied to constrain upper crustal cooling histories as rocks are exhumed to Earth's surface via a variety of geological processes. Collecting samples over significant relief (i.e., vertical profiles), and then plotting age versus elevation, is a long-established approach to constrain the timing and rates of exhumation. An exhumed partial annealing zone (PAZ) or partial retention zone (PRZ) with a well-defined break in slope revealed in an age-elevation profile, ideally complemented by kinetic parameters such as confined track lengths, provides robust constraints on the timing of the transition from relative thermal and tectonic stability to rapid cooling and exhumation. The slope above the break, largely a relict of a paleo-PAZ usually with significant age variation with change in elevation, can be used to quantify fault offsets. The slope below the break is steeper and represents an apparent exhumation rate. We discuss attributes and caveats for the interpretation of each part of an age-elevation profile, and provide examples from Denali in the central Alaska Range, the rift-flank Transantarctic Mountains, and the Gold Butte block of southeastern Nevada, where multiple methods reveal exhumed PAZs and PRZs in the footwall of a major detachment fault. Many factors, including exhumation rates, advection of isotherms and topographic effects on near-surface isotherms, may affect the interpretation of data. Sampling steep profiles over short-wavelength topography and parallel to structures minimises misfits between age-elevation slopes and actual exhumation histories.

P. G. Fitzgerald (✉)
Department of Earth Sciences, Syracuse University, Syracuse,
NY 13244, USA
e-mail: pgfitzge@syr.edu

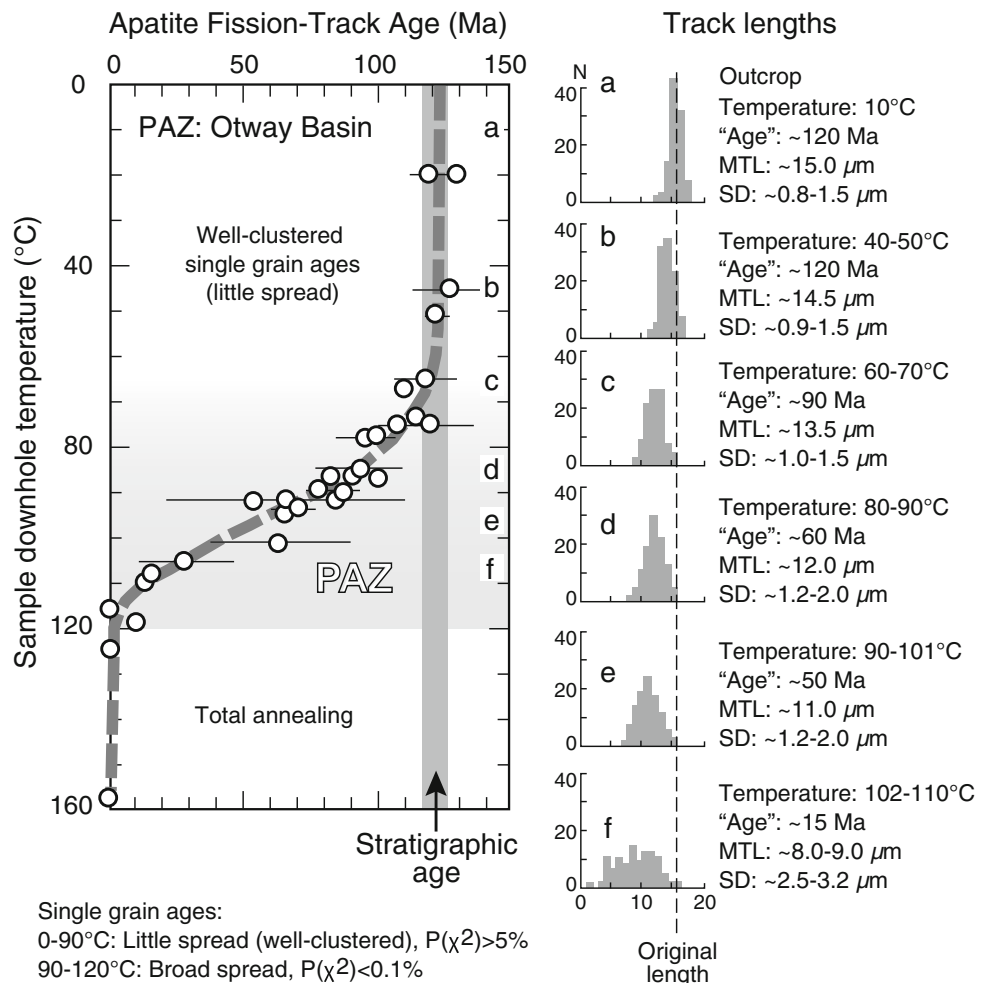
M. G. Malusà
Department of Earth and Environmental Sciences, University of
Milano-Bicocca, Piazza delle Scienza 4, 20126 Milan, Italy

9.1 Introduction

Thermochronology is the study of the thermal history of rocks and minerals. Thermochronologic ages are often interpreted as closure ages corresponding to a closure temperature T_c (Dodson 1973), which is defined as the temperature at which the system becomes closed, assuming monotonic cooling. Closure temperatures vary as a function of mineral kinetic parameters, cooling rate (T_c is higher for faster cooling), the composition of the mineral, and/or radiation damage of the crystal lattice (e.g., Gallagher et al. 1998; Reiners and Brandon 2006). In the case of low-temperature thermochronologic methods such as fission-track (FT) analysis, the simplest data interpretations are that thermochronologic ages record exhumation. This is because rocks cool as they move toward the surface of the Earth, i.e., as they are exhumed, either via tectonics and/or erosion.

Early FT studies (e.g., Naeser and Faul 1969) established that FT ages could be reset, or partially reset, due to temperature increases resulting from burial in a sedimentary basin or nearby igneous intrusions (e.g., Fleischer et al. 1965; Calk and Naeser 1973; Naeser 1976, 1981). Because temperature increases with depth, borehole studies (e.g., Naeser 1979; Gleadow and Duddy 1981) revealed that FT ages decreased with depth. In the case of apatite, borehole studies also revealed a zone of partial stability for fission-tracks corresponding to temperatures between ~ 120 and 60 °C (Fig. 9.1). This zone was initially called the “partial stability field” (Wagner and Reimer 1972) or “field of partial stability” (Naeser 1981), but other terms such as “partial stability zone” (Gleadow and Duddy 1981) or “track annealing zone” (Gleadow et al. 1983) were also used. Gleadow and Fitzgerald (1987) introduced the term *partial annealing zone* or PAZ, a term that has remained in common usage. The PAZ for apatite FT (AFT) and its characteristics are well defined in some boreholes (Fig. 9.1). AFT ages decrease downhole while single grain age dispersion tends to increase. Confined track length distributions also show

Fig. 9.1 Classic form of the partial annealing zone (PAZ) is shown in this compilation diagram showing downhole temperature versus AFT age for samples from the Otway Basin in SE Australia (summarised from Gleadow and Duddy 1981; Gleadow et al. 1986; Green et al. 1989; Dumitru 2000). Decreasing AFT ages and changing track length distributions with increasing downhole temperature reflect the changing rate of annealing, from very slow above ~60 °C, to increasing within the PAZ and then “geologically instantaneous” in the zone of total annealing



systematic trends—as distributions broaden downhole, mean lengths decrease and standard deviations increase (Gleadow and Duddy 1981; Gleadow et al. 1983; Green et al. 1986). These studies also documented the role of apatite composition in the rate of annealing, and hence the variable limits of the PAZ.

The PAZ can be defined as the temperature interval, corresponding to appropriate crustal depths, between where tracks are annealed geologically “instantaneously” and where they are retained without a significant loss in FT age on the geologic timescale. Annealing and track length reduction are more rapid at higher temperatures, but do continue, albeit much more slowly, even at ambient temperatures (e.g., Green et al. 1986). The same concept applies to other thermochronologic systems due to loss, or partial loss, via volume diffusion of daughter products, such as Ar in K–Ar systems (Baldwin and Lister 1998) and He in (U–Th)/He systems (Wolf et al. 1998). The term *partial retention zone* (PRZ) was introduced by these authors for these noble gas methods. We favour the use of PAZ for FT

thermochronology where annealing is the operative process for length reduction of individual tracks.

When samples are collected over significant relief, ages from different thermochronologic systems generally increase with increasing elevation. Age versus elevation plots, and the interpretation of age variations and slopes on these plots, marked a breakthrough for the earliest FT studies applied to tectonics (e.g., Wagner and Reimer 1972; Naeser 1976; Wagner et al. 1977). The slope of the age-elevation trend was initially interpreted as an “uplift rate,” but it is now clear that this trend provides information on the rate of *exhumation*, where exhumation is the displacement of rocks with respect to Earth’s surface (England and Molnar 1990). England and Molnar (1990) also defined the *surface uplift* as the displacement of the Earth’s surface (typically the mean surface elevation over an area) with respect to the geoid, and the *rock uplift* as the displacement of a rock with respect to the geoid (see Chap. 8, Malusà and Fitzgerald 2018a). Exhumation, surface uplift, and rock uplift are linked by the following relationship:

$$\text{Surface uplift} = \text{rock uplift} - \text{exhumation} \quad (9.1)$$

When the amount of exhumation and surface uplift can be independently constrained (i.e., because the paleo-mean land-surface elevation is known), rock uplift can also be constrained (Eq. 9.1). However, these situations are actually quite rare (e.g., Fitzgerald et al. 1995; Abbot et al. 1997). Moreover, it is important to emphasise that thermochronology does not constrain exhumation directly, because isotherms (the thermal reference frame) are controlled by a range of processes in the upper crust. The conversion from a thermal framework (which impacts the thermochronologic record) to a framework that constrains the timing and rates of exhumation requires assumptions about the dynamic thermal structure of the crust.

There are many factors that influence the slope of the age-elevation profile. Notably those related to the perturbation of the thermal structure of the crust associated with rapid exhumation, the shape of topography, or the way that samples are collected across the topography (e.g., Brown 1991; Brown et al. 1994; Stüwe et al. 1994; Mancktelow and Grasemann 1997). Many excellent papers and books discuss these topics in considerable detail (e.g., Braun 2002; Reiners et al. 2003; Braun et al. 2006; Reiners and Brandon 2006; Huntington et al. 2007; Valla et al. 2010; see also Chap. 8, Malusà and Fitzgerald 2018a; Chap. 10, Malusà and Fitzgerald 2018b; Chap. 17, Schildgen and van der Beek 2018). To plot thermochronologic ages versus elevation using an orthogonal coordinate system requires the fundamental assumption that data interpretation is one-dimensional (i.e., the particle path is vertical) and that samples are not collected laterally across the landscape. In essence, the vertical profile approach is the plotting of a three-dimensional data set in one dimension and coupled with the effects of advection of isotherms due to rapid exhumation often results in data misinterpretation.

In this chapter, we discuss the strategy of collecting samples over a significant elevation range to constrain the timing and rate of exhumation. We discuss the concept of the exhumed PAZ (or PRZ) and use a number of well-known examples to illustrate sampling strategies, common mistakes, factors, and assumptions that must be considered when interpreting thermochronologic data from age-elevation profiles.

9.2 Definition of a PAZ and PRZ

The classic form of a PAZ is shown clearly in AFT data plotted against depth (downhole temperature) from Otway Basin drill holes (Gleadow and Duddy 1981; Gleadow et al. 1983, 1986) (Fig. 9.1). The Otway Basin formed during the breakup between Australia and Antarctica and

was filled with >3 km volcanogenic sediments of the Lower Cretaceous Otway Group. The upper part of the AFT profile is defined by AFT ages of ~120 Ma, invariant down to a temperature of ~60 °C. Ages then decrease progressively, within the PAZ itself as the rate of annealing increases, down to a zero age at depths where the present temperature is ~120 °C. For the Otway Basin, the PAZ is therefore defined as between ~120 and ~60 °C. The chemical composition of the individual grains within the Otway Basin is variable, due to the volcanogenic provenance, with a mix of F-rich and Cl-rich grains (Green et al. 1985). Tracks within Cl-rich grains are more resistant to annealing (see Chap. 3, Ketcham 2018), so these grains reach a zero age at a higher temperature. The spread of single grain ages is the greatest at intermediate temperatures within the PAZ where the variable rates of annealing between grains of different chemical compositions are maximised (e.g., Green et al. 1986; Gallagher et al. 1998). Age dispersion within a PAZ is obvious when a downhole modeled-AFT age profile is plotted for Dpars of differing values (Fig. 9.2a). While not a direct proxy for chemical composition, Dpar—the diameter of track-etch figures measured parallel to the crystallographic *c*-axis—is commonly used as an indicator of the resistance of fission-tracks in apatite to thermal annealing (e.g., Burtner et al. 1994). In this example, the AFT age difference between a Dpar of 1 (fission-tracks are less resistant to annealing) and 3 (fission-tracks are more resistant to annealing) is ~45 Ma (~45% relative to the unannealed AFT age) at temperatures between 80 and 90 °C.

The variation of (U–Th)/He age with depth (temperature) is not discussed in detail in this chapter. However, formation of an apatite (U–Th)/He (AHe) age profile within a PRZ follows similar principles to those corresponding to an AFT PAZ. Note that there are slight differences in the shape of the modeled AHe PRZ versus the shape of the modeled-AFT PAZ at lower temperatures (Fig. 9.2), which reflect the different kinetics. In addition, the magnification of single grain age variations for AHe is even more pronounced within the PRZ, depending on the variation of effective uranium concentration [*eU*], grain size, zonation of the individual grains, and residence time within a PRZ (e.g., Reiners and Farley 2001; Farley 2002; Meesters and Dunai 2002; Fitzgerald et al. 2006; Flowers et al. 2009). Based on relative alpha particle production, [*eU*] is calculated as [*U*] + 0.235[*Th*] (e.g., Flowers et al. 2009). Figure 9.2b shows the age variation between a small grain with a low [*eU*] versus a large grain with a higher [*eU*] is ~70 Ma (~70% relative to unreset ages) at ~65 °C (held constant for ~100 Myr). This single grain age variation is a result of the grain size being the diffusion domain and the relative importance between loss via α -particle ejection and loss via volume diffusion, plus the effects of higher radiation

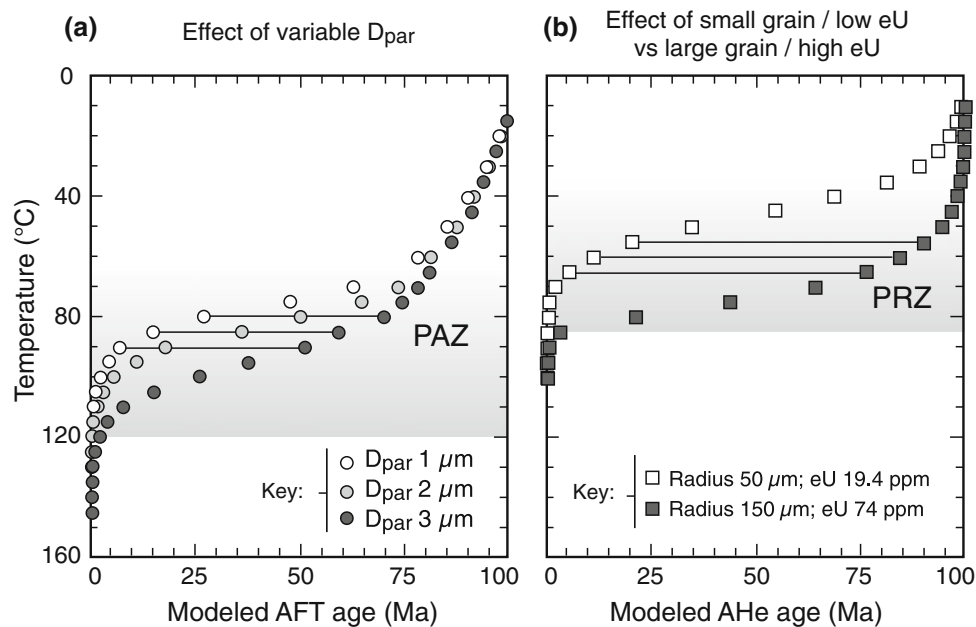


Fig. 9.2 **a** Effect of composition, using D_{par} as a proxy, on the variation of AFT ages within a PAZ. In these modeled examples, the differences in ages are observed for samples with D_{par} values of 1 and 3 μm . The greatest age dispersion lies in the interval 80–90 °C (marked by horizontal lines) where there is a ~40 Myr (40%) age difference between the two extremes. Age dispersion due to chemical composition is magnified by residence within, or slow cooling through, the PAZ. Modeled ages were produced using HeFTy (Ketcham 2005) and the Ketcham et al. (2007) annealing algorithm. **b** In a similar fashion, AHe age dispersion within a PRZ is

maximised when there is a mix of large grains/high [eU] (older grains) and small grains/low [eU] (younger grains). In this modeled scenario, the greatest difference in ages lies in the interval ~55–65 °C (marked by horizontal lines) where there is a ~70 Myr (70%) age difference. Age dispersion due to variable [eU] and grain size (plus zoning and other factors—not modeled here) is magnified by residence within, or slow cooling through the PRZ. Modeled AHe ages were produced using HeFTy (Ketcham 2005), the Flowers et al. (2009) algorithm and the Ketcham et al. (2011) α -particle ejection parameters

damage, in effect storing He inside damage zones within the crystal lattice (Reiners and Farley 2001; Farley 2002; Flowers et al. 2009). Age dispersion is more pronounced within a PRZ if grain zonation is such that the rim is depleted relative to the core (e.g., Meesters and Dunai 2002; Fitzgerald et al. 2006).

Confined track lengths are an essential component to the application of the PAZ concept to AFT thermochronology as they provide a kinetic parameter used to constrain the thermal history of each sample (e.g., Gleadow et al. 1986). Interpretations can be both qualitative (e.g., long mean lengths $\geq 14 \mu\text{m}$ indicate simple rapid cooling vs. more complex distributions that may reflect residence within a PAZ, slow cooling, or reheating) but also provide a fundamental input parameter to inverse thermal modeling (e.g., Ketcham 2005; Gallagher 2012; see Chap. 3, Ketcham 2018). Confined track length distributions (CTLDs) from the Otway Basin samples reveal the now well-established classic pattern of a PAZ, i.e., decreasing mean lengths and increasing standard deviations with increasing temperatures downhole (Fig. 9.1). These distributions reflect a shortening of tracks that have resided at the same crustal level and hence same temperatures for the last ~30 Myr (Gleadow

and Duddy 1981). Thus, in each case the maximum track length remains the same (reflecting the most recently formed confined track). But, as the rate of annealing increases with increasing temperature, the tracks anneal progressively faster and histograms broaden to reflect the annealing process. In this situation, track-length histograms can be imagined as conveyor belts; moving slowly from right to left when the temperature is low, and annealing slower near the upper part of the PAZ (i.e., leading to narrow distributions). Near the base of the PAZ (corresponding to higher temperatures), the conveyor belt is faster as the rate of annealing increases and CTLDs are broader. As mentioned above, compositional variation between apatite grains, particularly acute in Otway Basin sediments also leads to dispersion in downhole track lengths. In addition, anisotropic annealing of tracks in apatite (Green and Durrani 1977) where tracks perpendicular to the c -axis shorten faster than those parallel to the c -axis also leads to track length dispersion.

The shape and development of a PAZ (revealed in the AFT age-depth profile) are the result of a number of parameters including the thermal structure of the upper crust (i.e., the geothermal gradient) and the previous thermal and tectonic history (Figs. 9.1, 9.2 and 9.3). Typically, the

characteristic AFT age-depth trend formed in a PAZ, for example, as shown in the Otway Basin, is interpreted as a time of “relative tectonic and thermal stability,” with the upper part of the profile (<60 °C) reflecting the previous thermal history (i.e., formed in the geologic past). Within the PAZ, the slope of the AFT profile will vary as a function of the duration that samples have resided within the PAZ, the paleogeothermal gradient, and the relative thermal (and tectonic) stability at that time. The slope of the AFT-depth profile will be shallower if the PAZ forms over a long period of time (Fig. 9.3c). However, if samples are resident in the PAZ for only a short period of time, the variation in ages will not reflect the characteristic profile. If samples cool monotonically through the PAZ, then their AFT ages may be interpreted as closure ages representative of the time the sample cooled through the closure temperature T_c of the thermochronologic system under consideration (see Chap. 8, Malusà and Fitzgerald 2018a).

9.3 Vertical Profiles and the Exhumed PAZ/PRZ Concept

9.3.1 Recognition of an Exhumed PAZ

Thermochronologic data collected in age-elevation profiles from orogens may reveal simple linear relationships, and the T_c concept will apply (e.g., Reiners and Brandon 2006). However, depending on the level of erosion and the thermal/tectonic history, an exhumed PAZ may be revealed. This happens when a period of relative tectonic and thermal stability is followed by a period of rapid cooling and exhumation. Relative stability allows the development of the characteristic age-depth shape of a PAZ, which is then preserved in an age-elevation profile (Naeser 1979; Gleadow and Fitzgerald 1987) (Fig. 9.3a). The *break in slope* marks the base of a former PAZ, termed an *exhumed PAZ*, and approximates the onset of significant rapid cooling (Gleadow and Fitzgerald 1987; Fitzgerald and Gleadow 1988, 1990; Gleadow 1990). In essence, the break in slope represents a paleo ~ 110 °C isotherm, or whatever paleotemperature is appropriate given either the mineral composition or method under consideration. The significance of an inflection point in an age-elevation profile was first noted in the Rocky Mountains of Colorado (Naeser 1976). In an age-elevation profile from Mt Evans (4346 m), Chuck Naeser identified an inflection point at ~ 3300 m. This was interpreted as the former position of the ~ 105 °C isotherm, with the temperature based on Eielson (Alaska) drill hole age data (Naeser 1981; see Chap. 1, Hurford 2018). Naeser (1976) noted that “apatite below 3000 m reflects rapid uplift of the Rocky Mountains during the Laramide orogeny starting about 65 Myr ago,” whereas “apatite above 3000 m was

only partially annealed during the Cretaceous burial prior to the uplift.”

The slope above the break in slope (i.e., the exhumed PAZ) is not steep and reflects the shape of the former PAZ formed during a time of relative tectonic and thermal stability (Fig. 9.3c), rather than an apparent exhumation rate. However, the steeper slope below the break in slope represents instead an apparent exhumation rate—taking into consideration all the caveats that can modify the slope, as discussed below. With respect to the formation of the classic age profile within a PAZ, it is worth noting that it is unlikely to have formed within a period of “complete and absolute” tectonic and thermal stability. The thermal frame of reference is dynamic, for example, because of cooling associated with exhumation and/or relaxation of isotherms and even heating associated with subsidence and burial (see Chap. 8, Malusà and Fitzgerald 2018a). A simple way to envision an exhumed PAZ is by comparing the conditions during the formation of a PAZ relative to the time following that. In essence, the recognition of an exhumed PAZ is dependent on our ability to recognise different components within a track length distribution; those tracks annealed (and shortened) while the sample is resident in a PAZ and then long tracks that result from rapid cooling. To a certain extent, the exhumed PAZ concept can be demonstrated by comparing the gentler slope of an exhumed PAZ with the steeper slope of the age-elevation profile beneath the break. For example, in the Denali profile in Alaska (see Sect. 9.4.1), the slope of the exhumed PAZ above the break is ~ 100 m/Myr compared to the slope (apparent exhumation rate) below the break (~ 1500 m/Myr) (Fitzgerald et al. 1995). In the Transantarctic Mountains, slopes of exhumed PAZs are ~ 15 m/Myr compared to slopes (apparent exhumation rate) of ~ 100 m/Myr below the break (e.g., Gleadow and Fitzgerald 1987; Fitzgerald 1992). The slopes are different, but the relative durations for each (slow cooling and formation of the PAZ vs. rapid cooling) are about the same (3:1).

Track length measurements are crucial for interpreting thermal histories in general, but are also very useful for identifying exhumed PAZs. CTLDs from below the break in slope generally reflects rapid cooling (mean track length >14 μm , standard deviation <1.5 μm). CTLDs from above the break in slope reflects longer residence within the PAZ, with distributions often being bimodal, reflecting the two components of tracks (Fig. 9.3a). These distributions typically have means of ~ 12 – 13 μm with standard deviations of >1.6 μm . Within an exhumed PAZ, there will be a greater spread of single grain ages, because slower cooling magnifies differences arising between grains of different retentivity (Fig. 9.2). This concept is of fundamental importance to detrital thermochronology, where interpretation of single grain age data usually assumes that all ages represent closure

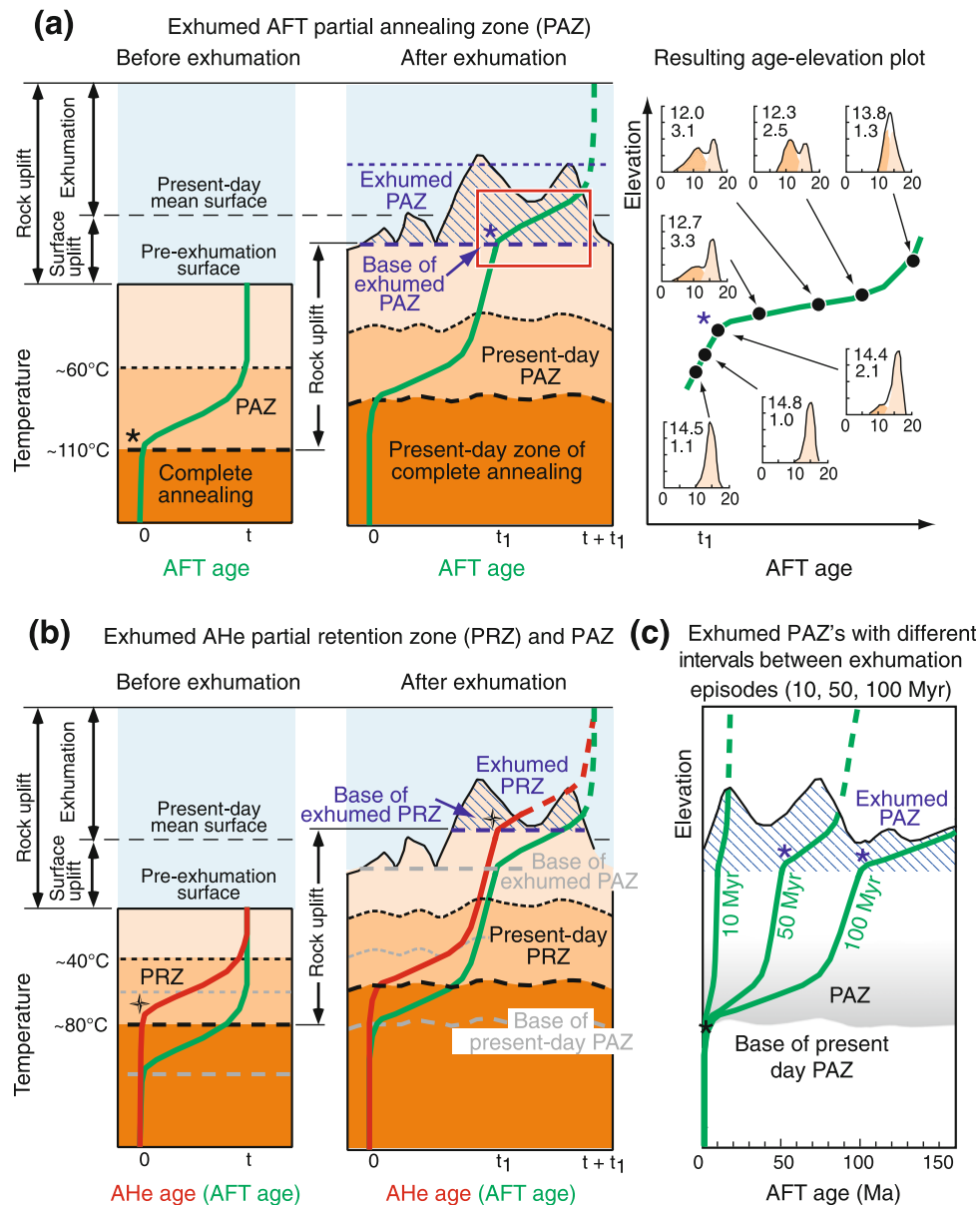


Fig. 9.3 **a** Concept of an exhumed AFT PAZ and the relationship between rock uplift, exhumation, and surface uplift. The left panel shows the characteristic shape of the AFT PAZ formed over the time period “ t ” during relative thermal and tectonic stability. Following a period of rock uplift, followed by exhumation and relaxation of the isotherms, an exhumed PAZ may be revealed in the age-elevation profile (middle panel). The asterisk marking the break in slope indicates the base of the exhumed PAZ and typically slightly underestimates the onset age of rock uplift as this point has to cool through the PAZ. Note that modeled isotherms mimic the surface topography. The right-hand panel shows the variation of track length distributions at various levels throughout the profile. Distributions below the break in slope contain only long tracks formed during rapid cooling with little time spent within the PAZ. In contrast, CTLDs

above the break in slope have shorter means and larger standard deviations as they contain two length components: pre-exhumation lengths (shortened due to annealing while resident within the PAZ) and long tracks that post-date the onset of rapid exhumation and have not been shortened due to annealing (modified from Fitzgerald et al. 1995). **b** The exhumed PAZ concept also applied to an exhumed AHe PRZ (marked by a cross) (modified from Fitzgerald et al. 2006). **c** An exhumed PAZ (or PRZ) will only be revealed in an age-elevation profile when there has been sufficient time between episodes of exhumation (e.g., 50 or 100 Myr in this example) to develop the classic form of a PAZ that represents a period of apparent thermal and tectonic stability. If the time period is too short, e.g., 10 Myr in this example, an exhumed PAZ will not be distinguishable (modified after Fitzgerald and Stump 1997)

ages, typically due to either rapid cooling via exhumation or cooling of volcanic rocks (e.g., Garver et al. 1999; Bernet and Garver 2005). In other words, the assumption in detrital

studies is that all thermochronologic ages are geologically meaningful. However, age variations observed in an exhumed PAZ (or PRZ) shows that this is not always the

situation. In many cases, only the age corresponding to the break in slope can be interpreted with respect to a geologic event. Lag-time calculations (thermochronologic age minus stratigraphic age) to constrain past exhumation rates may therefore be geologically meaningless if samples are eroded from within an exhumed PAZ (see below and Chap. 10, Malusà and Fitzgerald 2018b) because these ages do not represent closure ages and a large age dispersion exists within the exhumed PAZ.

A break in slope is drawn at the intersection of the lines representing the exhumed PAZ and the age-elevation profile below the break, although the base of a PAZ is actually a curve (Figs. 9.1, 9.2 and 9.3). This means that the time corresponding to the break in slope will slightly underestimate the timing of the onset of rapid cooling/exhumation. Also, samples close to the base of the PAZ will have to transit through the PAZ itself. Thus, if samples do not transit the PAZ rapidly, CTLDs will reflect more annealing (e.g., Stump and Fitzgerald 1992) and the age corresponding to the break in slope will slightly underestimate the true onset of rapid cooling/exhumation. Such a discrepancy may not be critical (i.e., not affect data interpretation) if an exhumed PAZ has a break in slope at ~ 50 Ma (for example). In this case, our ability to accurately locate the position of a break in slope is on the order of the precision of each age, so for a break in slope of ~ 50 Ma, it is on the order of $\pm 5\%$ for AFT. However, if a cooling event (and hence the time marked by the base of an exhumed PAZ) is Pliocene in age, distinguishing between the onset of cooling/exhumation at 6 or 4 Ma may be geologically significant.

In summary, the following factors affect the potential recognition of an exhumed PAZ (or PRZ) in an age-elevation profile:

- The period of relative thermal and tectonic stability prior to the initiation of more rapid cooling/exhumation. Sufficient time is in fact required to allow the shallow slope to develop (Fig. 9.3c).
- The magnitude of cooling/exhumation event that follows formation of the PAZ. If this is minor, then an exhumed PAZ will not be recognised. What is particularly important is the contrast in thermal and tectonic regimes between the formation of a PAZ and subsequent more rapid cooling/exhumation that preserves the classic PAZ form.
- When formation of a PAZ and subsequent cooling/exhumation occurred in the geologic record. If it occurred a long time ago, the precision of the dating method relative to the magnitude and duration of the geologic and/or tectonic event may not be adequate to reveal an exhumed PAZ, the exhumed PAZ may have been eroded away, or the proportion of shortened tracks (formed in the PAZ) to long tracks (subsequent to exhumation) may be insufficient to identify that period of relative stability,

even with modeling. In these cases, the interpretation of an age-elevation profile may be “slow or monotonic exhumation.” Models may also suggest a “good-fit” $T-t$ envelope that could be interpreted as “slow monotonous cooling,” but data precision may be insufficient to reveal different events. An important point is that data and models must be interpreted within a geologic context. Geologic events are by their very nature episodic whether on the temporal scale of earthquakes or volcanoes, during times of accelerated mountain building or part of an orogenic cycle. The same analogy applies to different thermochronologic methods. Higher temperature methods tend to only reveal major events and often indicate “monotonous cooling,” whereas the lower temperature methods may reveal individual events. Of course, lower temperature techniques are more susceptible to the effects of dynamic isotherms (e.g., Braun et al. 2006).

We have only discussed an exhumed PAZ with respect to the age of the break in slope as representing cooling due to exhumation, usually associated with rock uplift. However, in rapidly deforming orogens (e.g., Himalaya, Taiwan, and Southern Alps of New Zealand) a break in slope may also be revealed on a multi-method plot of age versus temperature, for analyses performed on the same sample (Kamp and Tippet 1993; Ching-Ying et al. 1990). Such a break is usually interpreted in terms of the onset of a major tectonic/exhumation/cooling event. However, because isotherms are perturbed during such rapid exhumation, the data may be equally well explained by a constant exhumation rate leading to an exponential decrease in temperature with time (Batt and Braun 1997; Braun et al. 2006).

The ultimate test of any thermochronologic interpretation involves comparison with the geologic record. For example, does an inflection point on either a single-method age versus elevation plot, or in a multi-method age versus temperature plot, represent relaxation of compressed isotherms or cooling due to erosion/exhumation due to uplift and creation of relief in an active (or recently inactive) orogen? If there is a nearby sedimentary basin with a large influx of detritus (e.g., conglomerates) that were the same age as that associated with the inflection point, this would provide evidence for an interpretation of cooling due to exhumation as opposed to relaxation of compressed isotherms.

9.3.2 Attributes and Information to Be Gained from an Exhumed PAZ

In previous sections, we discussed the characteristics of a PAZ and the recognition of an exhumed PAZ. In this section, we discuss the attributes of, and the information that can be obtained from an exhumed PAZ (Fig. 9.4), as further

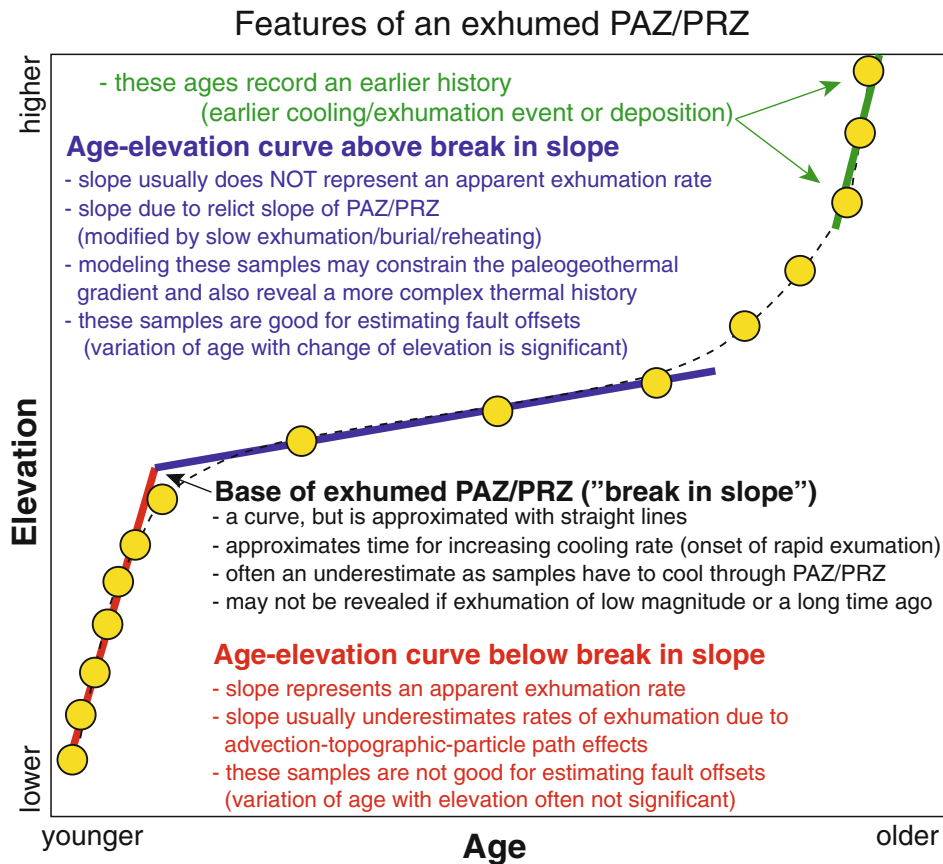


Fig. 9.4 Summary of the attributes and information available from an exhumed PAZ/PRZ

illustrated in Sect. 9.4 with examples from Denali, the Transantarctic Mountains and the Gold Butte Block.

Timing of Exhumation As mentioned above, the time corresponding to the break in slope represents the transition from a relatively stable thermal and tectonic regime to a time of more rapid cooling, usually related to exhumation as a result of rock uplift. The break in slope will underestimate the “true” time of transition, because of the geometry of the curve and because rocks take time to transit the PAZ. Inverse thermal modeling (see Chap. 3, Ketcham 2018) for samples just above the break in slope will reveal a period of residence within the PAZ, followed by the onset of rapid cooling. Inverse thermal modeling for samples below the break in slope typically will reveal rapid cooling only, but not the onset of rapid cooling. During the transition from relative thermal and tectonic stability to rapid exhumation, the evolving thermal regime can be complex, before steady state may become established. Higher temperature thermochronometers are slower to respond and establish steady state than low-temperature systems (e.g., Reiners and Brandon 2006). In a modeling paper, Moore and England (2001) found that in the case of a sudden increase in the rate of cooling due to erosion, the advection of isotherms means that the recorded ages only show a gradual increase in the

rate of exhumation. Valla et al. (2010), in another modeling paper, discuss in detail the effect that changes in relief have on the resolution of thermochronologic data sets. They conclude that changes in relief can only be quantified and constrained if the rate of relief growth exceeds $\sim 2\text{--}3$ times the background exhumation rate. The bottom line is that if there are detectable variations in an age-elevation profile such as an exhumed PAZ, then these variations are significant and meaningful as regards the geologic and landscape (relief, topography) evolution.

Amount of Exhumation Because an exhumed PAZ corresponds to a time of relative stability, it is reasonable to assume that the geothermal gradient was also relatively stable. Thus, assuming a reasonable paleogeothermal gradient (typically between 20 and 30 °C/km representing a relatively stable continental geotherm) allows one to convert the paleotemperature at the base of the exhumed PAZ (e.g., ~ 110 °C) to the amount of rock removed. Depending on the elevation of the break in slope relative to the mean land-surface elevation, the amount of exhumation since the time of the break in slope can be estimated (see Brown 1991; Gleadow and Brown 2000). Thus, an average rate of exhumation since the timing of the break can be constrained

and, if appropriate, this rate can be compared to the apparent exhumation rate based on the age-elevation slope below the break. If the stratigraphy (above the break) or rock removed can be reconstructed or independently constrained, then the paleogeothermal gradient can also be constrained, as for the Transantarctic Mountains in the Dry Valleys area (Gleadow and Fitzgerald 1987; Fitzgerald 1992). As the depth to the base of a PAZ is usually 3–5 km (being a function of paleogeothermal gradient), it is possible to design a sampling strategy, based on geological constraints or other information that is aimed at collecting an age-elevation profile that has an exhumed PAZ, purely because it does provide such a useful marker.

The Slope of the Exhumed PAZ The slope of this part of the profile (i.e., above the break in slope) does not typically represent an apparent exhumation rate. Viewed in one dimension, the slope depends on the factors discussed above (length of time over which the PAZ formed, paleogeothermal gradient) and the relative thermal stability both when the PAZ was formed and since rapid cooling began (approximated by the time corresponding to the break in slope). Inverse thermal modeling of samples over an elevation range can constrain the paleogeothermal gradient (see Chap. 8, Malusà and Fitzgerald 2018a). A factor in mathematically constraining the slope of the profile, both above and below the break in slope, is often the relatively large uncertainties (compared to the number of analyses) for AFT ages or the variation of single grain ages for AHe ages. This explains why age-elevation slopes are often determined as a line of best-fit “by eye,” in addition to calculating least-square regression lines.

The Exhumed PAZ as a Tectonic Marker As mentioned above, low-temperature thermochronologic ages are very useful as tectonic markers because there may be systematic variation of age with elevation (e.g., Wagner and Reimer 1972). As such, this concept is often called “fission-track stratigraphy (Brown 1991). Notably, sample ages within an exhumed PAZ typically vary significantly with elevation changes and thus are more useful as tectonic markers in contrast to sample ages below a break in slope where ages may be concordant within error over considerable topographic relief (see Chap. 10, Malusà and Fitzgerald 2018b; Chap. 11, Foster 2018).

9.3.3 Attributes and Information to Be Gained from the Age-Elevation Profile Below the Break in Slope

The slope of the age-elevation profile below a break in slope is generally steep and CTLDs indicates rapid cooling. Samples spend little time within a PAZ as they cool rapidly

through it, and ages can be interpreted as closure temperature ages. As compared to the slope of the exhumed PAZ, this part of the profile is often more typical of what is often found in mountain belts, with the slope representing an *apparent exhumation rate*. Typically, the slope overestimates the real exhumation rate due to a combination of advection and isotherm compression, the effect of topography on near-surface isotherms, and where samples are collected across the topography or the topographic wavelength (Brown 1991; Stüwe et al. 1994; Brown and Summerfield 1997; Mancktelow and Grasemann 1997; Stüwe and Hintermüller 2000; Braun 2002, 2005; Ehlers and Farley 2003; Braun et al. 2006; Huntington et al. 2007; Valla et al. 2010).

The reference frame against which we plot the age of samples (i.e., the elevation, altitude or depth, E in Fig. 9.5a) is not necessarily representative of the thermal frame of reference where the samples acquire their thermochronologic signature (Z in Fig. 9.5b–e). When plotting age versus elevation, the assumption is that the reference frame, i.e., isotherms were horizontal, and that samples have been exhumed vertically. However, isotherms mimic topography, albeit in a dampened fashion, with the impact of relief on isotherms becoming less with greater depth (e.g., Stüwe et al. 1994; see Chap. 8, Malusà and Fitzgerald 2018a). The depth to relevant isotherms is greater under ridges and less under valleys. The slope (apparent exhumation rate) of an age versus elevation profile in this situation will overestimate the true exhumation rate because ΔZ is less than ΔE (Fig. 9.5b). In the situation where exhumation is rapid and isotherms are compressed, the slope (the apparent exhumation rate) of the age-elevation profile will also overestimate the true exhumation rate (Fig. 9.5c). The wavelength of the topography matters, although the relief does not (Reiners et al. 2003), with a greater wavelength (a wider valley) having a greater effect on the slope of the age-elevation profile than a shorter wavelength (a narrow valley). In the situation where advection has not compressed the isotherms, it is possible to correct the slope of the age-elevation profile for topographic effects. This correction can be made for different T_c isotherms and hence is relevant for different thermochronologic techniques. Using the admittance ratio (α : the ratio of isotherm depth to topographic relief; Braun 2002), Reiners et al. (2003) presented a method to correct the apparent slope. The wavelength of topography is measured, and with respect to an appropriate closure isotherm, the admittance ratio (which is independent of topographic relief) is graphically determined. The assumption in these situations is that the paleotopography at the time when the ages were recorded has remained the same as it is today. An example: if $T_c = 100$ °C and the wavelength of topography is 10 km, then $\alpha = 0.1$. The slope (apparent exhumation rate) of the age-elevation plot is multiplied by $(1 - \alpha)$ to yield a “true exhumation rate.” If the measured slope is ~ 150 m/Myr, then the exhumation rate is $150 \times (1 - 0.1) = \sim 135$ m/Myr. The

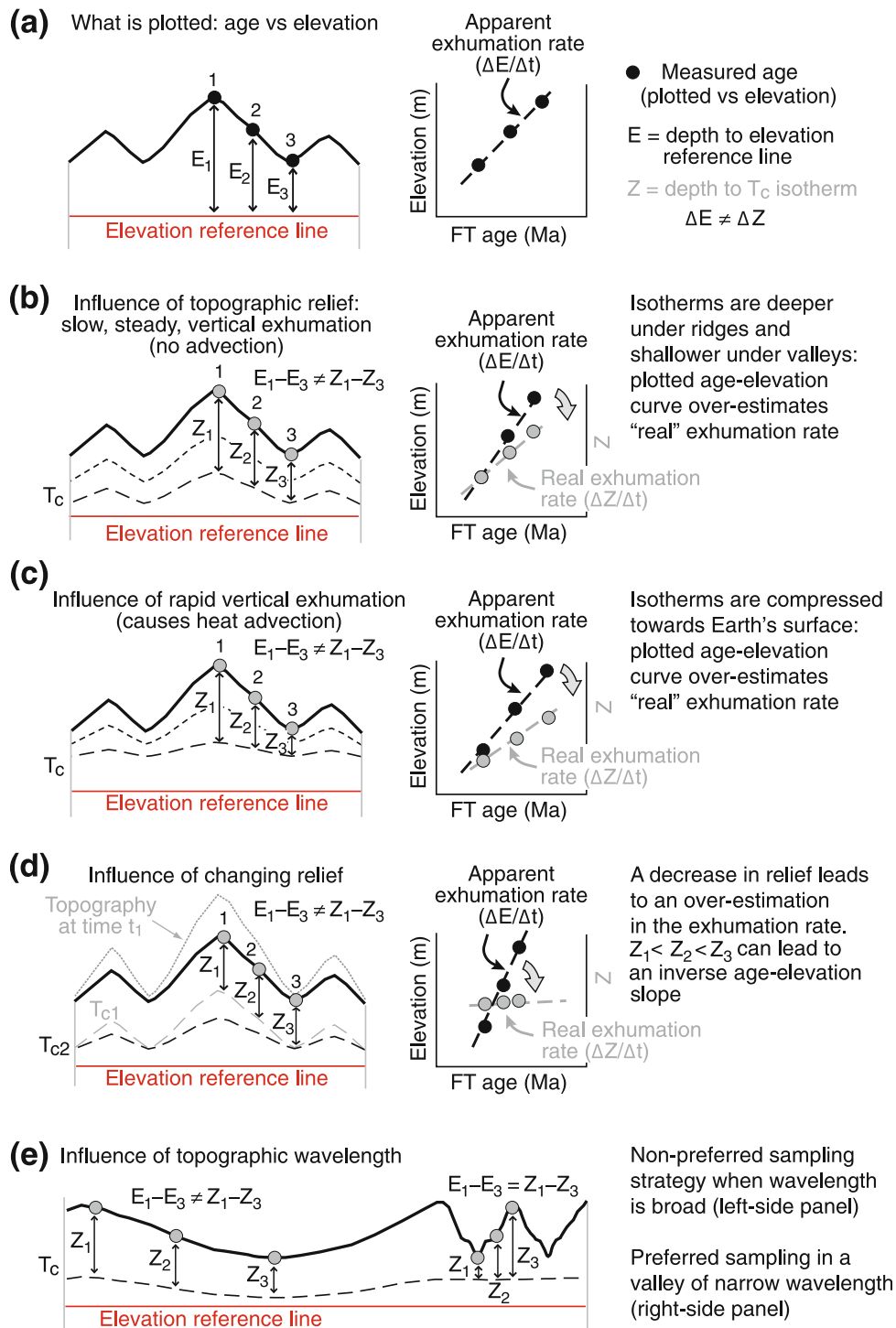


Fig. 9.5 Age-elevation scenarios, summarised from Stüwe et al. (1994), Mancktelow and Grasemann (1997), and Braun (2002). **a** The simple age-elevation model where ages are plotted against elevation. Implicit assumptions are that the thermal reference frame is horizontal, that ages reflect closure through a certain T_c , and that the particle path is vertical. The slope of the line is the “apparent exhumation rate.” **b** The effects of topography on the subsurface isotherms. The depth to T_c isotherms is deeper under ridges than under valleys. As samples are not collected vertically, the plotted 1D age-elevation apparent exhumation rate will be an overestimate of the “real” exhumation rate. The topographic effect is more pronounced

for low-temperature techniques than high temperature methods due to the greater deflection of the isotherms at shallow levels. **c** The effects of topography on the subsurface isotherms where exhumation is rapid, and isotherms are advected toward Earth’s surface and compressed. The plotted 1D age-elevation apparent exhumation rate is an overestimate. **d** If surface topography changes dramatically over time, this will lead to an overestimation of the “true exhumation rate,” plus in cases where $Z_1 < Z_2 < Z_3$, an inverse age-elevation relationship may also be recorded. **e** Vertical sampling profiles ideally should be collected from short-wavelength topography over the minimal horizontal distance

correction is greater for lower temperature techniques. Note however that the significance of being able to distinguish between a ~ 150 m/Myr apparent exhumation rate and a ~ 135 m/Myr exhumation rate, given the precision of individual ages and uncertainties on the age-elevation slope may be debatable. However, should there be age-elevation data from different techniques and with differing slopes; correcting these using this method may resolve the difference, with corrected slopes being similar.

The dimensionless Peclet number (Pe) can be used to quantitatively establish whether advection is the dominant form of heat transport (which will modify the age-elevation relationship) as compared to conduction (Batt and Braun 1997; Braun et al. 2006):

$$Pe = \dot{E}L/\kappa \quad (9.2)$$

where \dot{E} = exhumation rate (km/Myr), L = thickness of the layer being exhumed (km), κ = thermal diffusivity of crustal rocks (km^2/Myr). If Pe is much greater than 1, advection dominates, but if it is much less than 1, conduction will dominate.

There is a general rule to evaluating whether advection has played a role in the modification of the age-elevation slope. Not including the effects of topography, but if the slope of an age-elevation profile is less than ~ 300 m/Myr (Parrish 1985; Brown and Summerfield 1997; Gleadow and Brown 2000), then advection is likely not a factor (also see Reiners and Brandon 2006, their Fig. 3).

In the situation where surface topography has evolved with time (Fig. 9.5d), where there has been a change of relief, the slope of the age-elevation profile will still overestimate the exhumation rate (Braun 2002). In extreme cases where $Z_1 < Z_2 < Z_3$, the slope of the age-elevation profile, collected over long-wavelength topography, may be inverted, and younger ages are found at higher elevations and older ages are found at lower elevations, even in the case where there is no observed fault offsets between samples. Note that in the same region, if a vertical sampling profile was collected from a cliff (representing short-wavelength topography), the slope of the age-elevation profile would be positive and the slope would represent an apparent mean exhumation rate (Braun 2002). Thus, collecting samples across topography with different wavelengths has the potential to yield different age-elevation relationships that may be interpreted quite differently, but yet have formed under similar conditions (Fig. 9.5e).

Development of sampling strategies and understanding various factors that affect the age-elevation relationship are critical for data interpretation. To augment geologic interpretations of thermochronologic data, quantitative modeling

methods utilizing the heat transport equation can be used to constrain the rate of landscape evolution, that is, the shape of the surface topography and the rate at which it evolves (Braun 2002). Application of such methods usually requires sampling across different wavelengths on a regional scale. Quantitative modeling methods, such as the finite element code PeCube (Braun 2003) are powerful techniques, not only for interpreting existing data sets, but also for exploring the effects that exhumation (at different rates) and changing relief (constant, increasing, decreasing) have on the age-elevation relationship (e.g., Valla et al. 2010).

In the above discussion (and in Fig. 9.5), the assumption is that samples are exhumed vertically, and it is the rate of exhumation, the shape (and evolution) of topography, and the advection of isotherms that are the significant influences on the age-elevation relationship. However, samples are not always exhumed vertically, especially in areas of convergence where thrusting may play a role (e.g., ter Voorde et al. 2004; Lock and Willett 2008; Huntington et al. 2007; Metcalf et al. 2009). Notably, thrusting does not exhume rocks. It is erosion following the formation of topography during thrusting that exhumes and cools the rocks. Therefore, exhumation paths may have a significant lateral component. In this situation, the rock has a longer pathway to the surface, and this will affect the estimate of the exhumation rate. Huntington et al. (2007) explored this effect using a 3D finite element model, with topography modeled on the Himalaya. They also found that the shape of the isotherms as constrained by the shape of the orogen is important. Orogens are usually curvilinear in map view, with orogen perpendicular isotherms bent more than isotherms in a plane parallel to the orogen. With respect to vertical exhumation, the slope of the age-elevation profile from samples collected from gentle topographic slopes in the plane perpendicular to the orogen will overestimate considerably the “true” exhumation rate, dependent on rate of exhumation, topographic slope, and thermochronologic method used. For methods with lower T_c such as the AHe method, the apparent slope of the age-elevation profile can be much greater than the true exhumation rate. The discrepancy between the true modeled rate and the apparent slope is minimised when samples are collected from steeper topographic slopes and from age-elevation profiles oriented parallel to the trend of the mountain belt.

Different terminology may be used when samples are collected over considerable relief. “Vertical profile,” “age-elevation profile,” or “age-elevation relationships” (AER) are common. However, unless from a drill hole, samples collected over significant relief are never vertical, no matter how steep the side of a mountain may seem when

sampled. Many factors, as discussed above, affect the slope and interpretation of an age-elevation profile, and it is important to design a sampling strategy appropriate to the questions being addressed. Some studies, for example, collect samples over a wide region, but may also plot ages versus elevation, to take advantage of the AER. In this case, care must be taken in data interpretation because samples do not likely fit the ideal age-elevation sampling criteria. The criteria can be summarised as: samples should be collected over significant relief, over a short horizontal distance, in short-wavelength topography and have, if possible, the profile oriented parallel to the trend of the mountains and not cross any known (or unknown) faults. In general, samples collected from young and active orogens (e.g., Himalaya—van der Beek et al. 2009) will yield young ages, heat advection must be taken into consideration as isotherms will be compressed, ages from thermochronologic methods with different T_c may be concordant, and an exhumed PAZ may only be preserved in the highest elevations dependent on the level of erosion. In this situation, the slope of the age-elevation profile is likely to greatly overestimate the true exhumation rate.

9.4 Examples of Exhumed PAZs and PRZs

In this section, we briefly introduce three examples where exhumed PAZs, and in some cases exhumed PRZs, are well exposed in age-elevation profiles. Each example offers data interpretation subtleties. The presentation of the data and the interpretations are based largely on the papers where these examples were first presented, but in some cases, there is more known about the geology or there is new thermochronologic information. Where appropriate, we briefly discuss the integration of new data while keeping within the objectives of the chapter.

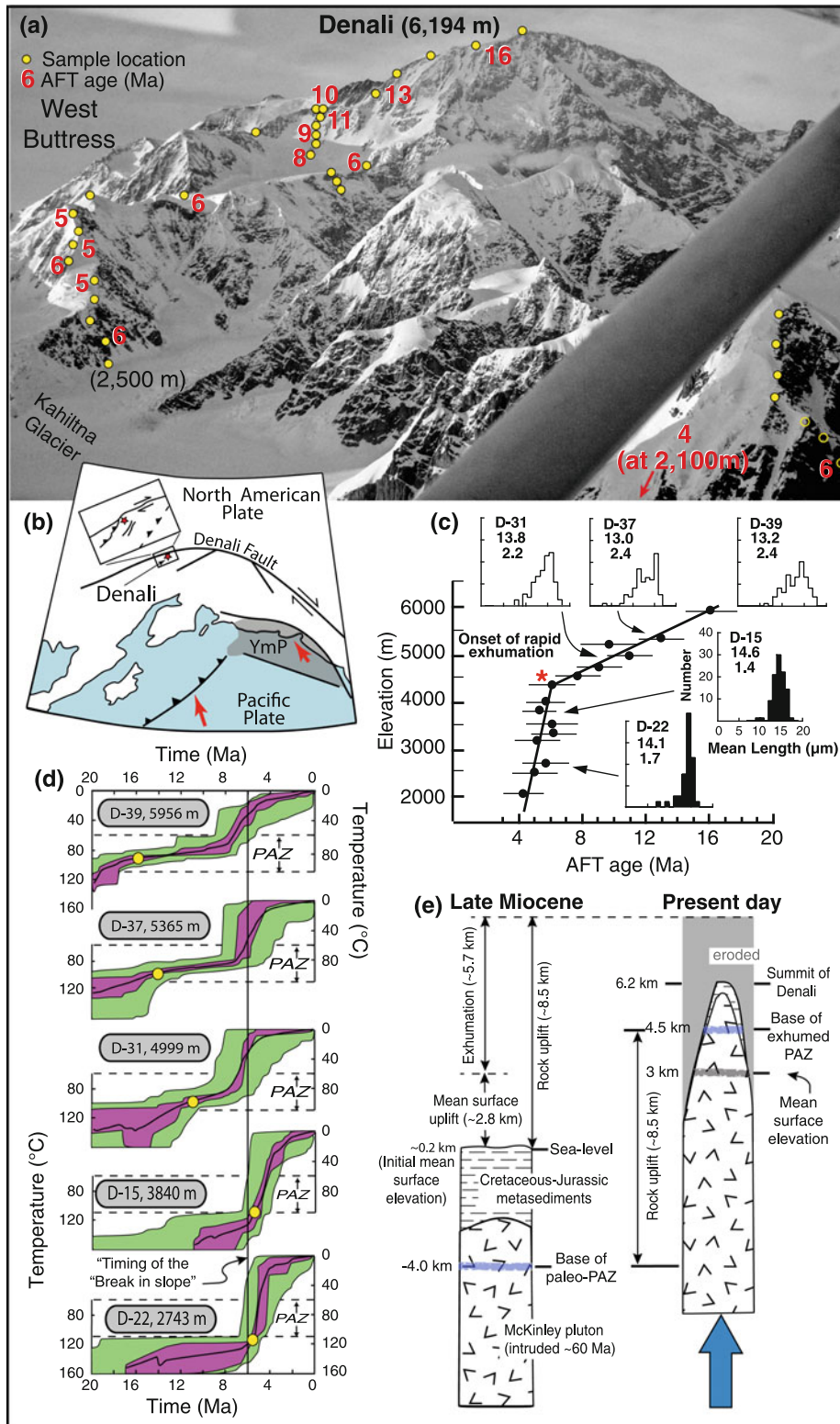
Fig. 9.6 **a** Photograph of the southwestern flank of the Denali massif with sample locations (hollow dot means the sample is on the other side of the ridge) and AFT ages. Photograph by Paul Fitzgerald. **b** Tectonic sketch map of southern Alaska. YmP = Yakutat microplate. Modified from Haeussler (2008). **c** AFT age ($\pm 2\sigma$) versus elevation profile collected from the western flank of Denali. Representative CTLDs are shown with sample numbers, mean length (e.g., 13.8 μm) and standard deviation (e.g., 2.2 μm). The red asterisk marks the base of an exhumed PAZ and indicates the onset of rapid exhumation. CTLDs below the break in slope have long means ($>14 \mu\text{m}$) indicative of rapid cooling. In contrast, those above the break typically have shorter means, larger standard deviations, and more complex histograms often being bimodal, indicative of residence within the PAZ prior to rapid cooling (modified from Fitzgerald et al. 1993, 1995). **d** HeFTy inverse thermal models of select Denali samples. Good-fit paths lie within the magenta envelope and acceptable fit lie within the green envelope (see Ketchum 2005 for definitions). Modeling constraints are loose (a higher temperature $T-t$ box and an ending low-temperature box) but c -axis projections for length measurements were not used on these original data from Fitzgerald et al. (1993,

9.4.1 Denali Profile (“Classic” Vertical Profile)

Denali, the highest mountain (6194 m) in the central Alaska Range and in North America, lies on the southern (concave) side of the McKinley restraining bend of the continental-scale right-lateral Denali fault system (Fig. 9.6a, b). Pacific–North American plate boundary forces in southern Alaska transfer stress inland causing slip along the Denali Fault (e.g., Plafker et al. 1992; Haeussler 2008; Jadamec et al. 2013). Stress is partitioned into fault-parallel and fault-normal components, with thrusting creating topography mainly at the restraining bends, to form the high mountains of the Alaska Range. Contrasting rheological properties of juxtaposed tectonostratigraphic terranes and suture zones formed during Mesozoic terrane accretion also play a role in the location of the highest topography and greatest exhumation (Fitzgerald et al. 2014). The Denali massif is largely defined by a granitic pluton, intruded at ~ 60 Ma into country rock comprised largely of fine-grained Jurassic–Cretaceous metasediments (e.g., Reed and Nelson 1977; Dusel-Bacon 1994). The summit and upper ~ 100 m of the mountain form a roof-pendant of these metasediments. The topography of the central Alaska Range is to a large extent defined by the erodibility of metasediments relative to the more resistant granitic plutons, as well as the relationship of the Denali Fault and the location of thrust faults (e.g., Fitzgerald et al. 1995, 2014; Haeussler 2008; Ward et al. 2012).

On the steep western flank of Denali, a vertical sampling profile covering ~ 4 km of relief was collected from near the summit to the base of Mt Francis (Fig. 9.6a, c). As discussed above, sampling profiles are rarely vertical and even in such a steep and topographically impressive massif as Denali, the average slope along the sampling profile, between the summit and the base of Fission Ridge at 2500 m, is $\sim 24^\circ$. Approximately 45 samples were collected in this profile. An initial reconnaissance suite of 15 samples produced a

1995), and an average Dpar per sample (not per grain counted or each length measured) was applied. Yellow dots indicate the AFT age. Rapid cooling for higher elevation samples starts ~ 1 Myr before the onset of rapid cooling/exhumation for those samples closer to the ~ 6 Ma break in slope. **e** Diagram modified from Fitzgerald et al. (1995) showing the schematic late Miocene (prior to significant uplift) and present-day rock columns. By using geomorphic and sedimentological constraints, the late Miocene paleo-mean surface elevation (~ 0.2 km) was estimated, which allows the amount of surface uplift to be calculated as ~ 2.8 km (the present-day mean surface elevation is ~ 3 km). The depth to the base of the paleo-PAZ was estimated as ~ 4 km (using a pre-uplift paleogeothermal gradient of $\sim 25^\circ\text{C}/\text{km}$)—and hence, as the base of the exhumed PAZ is now at ~ 4.5 , ~ 8.5 km of rock uplift has occurred since the late Miocene. The amount of exhumation was estimated using Eq. 9.1 which yields ~ 5.7 km ($2.8 = 8.5 - 5.7$ km). Exhumation using the method of Brown (1991) yields ~ 5.75 km. Geological constraints and uncertainties on all of these figures are discussed in Fitzgerald et al. (1995). The summit of Denali was estimated to be 2.1–3 km below the surface in the late Miocene prior to the onset of significant uplift



well-defined age-elevation profile (Fig. 9.6c), and the remaining samples were not processed. The uppermost sample, collected at the top of the Cassin Ridge, very close to the top of the pluton near the lithologic boundary with the metasediments, did not yield apatites, most likely because it was near the very edge of the pluton.

AFT ages decrease from ~ 16 Ma near the summit of Denali (~ 6 km elevation) to ~ 4 Ma at ~ 2 km elevation (Fig. 9.6c). A distinctive break in slope at ~ 6 Ma occurs at an elevation of ~ 4.5 km. Below this break in slope, for ages < 6 Ma, CTLDs have means > 14 μm and small standard deviations reflecting rapid cooling, although a few shorter tracks are present. Above this break in slope, samples with ages > 6 Ma have CTLDs with means of ≤ 13.5 μm and larger standard deviations. These broader distributions, bimodal in cases, reflect shortening of older tracks while resident within a PAZ, in addition to the tracks formed after ~ 6 Ma that are long and reflect rapid cooling. Fitzgerald et al. (1993, 1995) interpreted this break in slope as the base of an exhumed AFT PAZ, in effect representing the paleo ~ 110 $^{\circ}\text{C}$ isotherm, and reflecting the transition from a time of relative thermal and tectonic stability to a time of rapid cooling, due to rapid denudation as a result of rapid rock uplift and formation of the central Alaska Range beginning ~ 6 Ma (see discussion below).

Inverse thermal models undertaken using HeFTy (Ketchum 2005) are presented in Fig. 9.6d. These models confirm the qualitative interpretation above—long-term residence associated with slow cooling through the PAZ with rapid cooling beginning ~ 6 Ma. The modeled rate of cooling for the older samples above the break in slope at ~ 6 Ma is 2–3 $^{\circ}\text{C}/\text{Myr}$, much slower than the modeled cooling rates for samples below the break, which are up to ~ 50 $^{\circ}\text{C}/\text{Myr}$. Samples below the break in slope will not necessarily indicate rapid cooling began at ~ 6 Ma, for the very reason that these samples lie below the break in slope and hence started to cool after ~ 6 Ma. The good-fit T - t envelopes for samples above the break suggest rapid cooling may have started closer to ~ 7 Ma or even ~ 8 Ma for the uppermost sample.

The elevation of the break in slope, in conjunction with a paleogeothermal gradient of ~ 25 $^{\circ}\text{C}/\text{km}$ —estimated for the time of relative thermal and tectonic stability prior to the onset of rapid exhumation—was used to constrain the amount of exhumation at Denali since the late Miocene to ~ 5.7 km. Gallagher et al. (2005) in their modeling study (see below) estimated the paleogeothermal gradient at Denali in the late Miocene as 24.7 $^{\circ}\text{C}/\text{km}$. Fitzgerald et al. (1995) used geomorphic and sedimentological information to constrain the mean land-surface elevation in the late Miocene to ~ 0.2 km. This allowed the late Miocene to recent amount and average rates of the following to be constrained at Denali (Fig. 9.6e): rock uplift (~ 8.5 km with an average rate of ~ 1.4 km/Myr), exhumation (~ 5.7 km with an average rate of ~ 1 km/Myr),

and surface uplift (~ 2.8 km with an average rate of ~ 0.5 km/Myr). The summit of Denali was approximately 2.1–3 km below the surface prior to late Miocene rapid exhumation, estimated by subtracting the difference between the elevation of the break in slope (4.5 km) and the summit elevation (6.2 km) from the depth below the surface of the base of the PAZ in the Miocene (3.8–4.7 km). A “horizontal” sampling transect collected near-perpendicular to the Denali Fault and across the central Alaska Range yielded progressively older AFT ages up to ~ 37 Ma (Fitzgerald et al. 1995). With that trend, assuming that the slope of the age-elevation plot for samples > 6 Ma maintained the same gentle slope for these older samples, the amount of rock uplift, exhumation, and surface uplift decreased to values of ~ 3 , ~ 2 , and ~ 1 km on the southern side of the range.

The slope of the profile (~ 160 m/Myr) above the break at ~ 6 Ma represents an exhumed PAZ and as such does not represent an apparent exhumation rate. However, this slope was regarded by Fitzgerald et al. (1995) as being slightly too steep to represent a completely stable thermal and tectonic situation, and they interpreted this part of the profile as cooling at < 3 $^{\circ}\text{C}/\text{Myr}$. The apparent slope of the profile for samples younger than ~ 6 Ma (< 4.5 km elevation) is ~ 1.5 km/Myr, steep enough that heat advection is likely significant. To confirm this, a Peclet number can be estimated (see Sect. 9.3.3). We use a layer thickness of ~ 35 km, which represents crustal thickness south of the central Alaska Range, rather than the crustal thickness under the range which is ~ 35 –45 km (e.g., Veenstra et al. 2006; Brennan et al. 2011). This plus a thermal diffusivity of 25 km^2/Myr and an exhumation rate of ~ 1 km/Myr yields a Peclet number of 1.4. Thus, the slope of the age-elevation profile below the break overestimates the exhumation rate, due to advection as well as topographic effects (see Fig. 9.5).

Gallagher et al. (2005) used the Denali data as a test case when modeling multiple samples in vertical profiles to constrain the maximum likelihood thermal history. They used a Markov chain Monte Carlo (MCMC) approach with a Bayesian test criteria to test for over-parameterisation and complexity to the thermal history. The results of that modeling confirmed the interpretation of age and track length data, i.e., slow cooling followed by an inferred increase in cooling rate between 7 and 5 Ma. When modeled individually, the higher elevation samples tended to imply the onset of rapid cooling were slightly earlier, as was the case for the HeFTy models presented in Fig. 9.6d.

The Denali AFT age-elevation profile has stood the test of time well. The simple interpretation of an exhumed PAZ representing a relatively stable thermal and tectonic setting prior to the onset of rapid cooling due to rock uplift and exhumation beginning in the late Miocene (~ 6 Ma) remains essentially unchanged. However, more thermochronological data from other parts of the Alaska Range along the Denali

Fault reveal episodic cooling, with strong episodes beginning at ~ 25 and ~ 6 Ma, and slightly less predictable and often weaker episodes in the middle Miocene (~ 15 to ~ 10 Ma) (e.g., Haeussler et al. 2008; Benowitz et al. 2011, 2014; Perry 2013; Riccio et al. 2014; Fitzgerald et al. 2014). These episodic cooling events are inferred to result from the effects of plate boundary processes at the southern Alaska margin. These include collision of the Yakutat microplate, shallowing of the Yakutat slab that results in stronger coupling with the overriding North America plate, and changing relative plate motion between the Pacific and North American plates. In addition, in places Cretaceous cooling is revealed in low-temperature thermochronology data, possibly associated with early development of the Denali Fault. There is a strong ~ 50 and 40 Ma thermal signal in the regional data set that may be due to progressive east-to-west ridge subduction along the southern Alaskan margin (e.g., Trop and Ridgway 2007; Benowitz et al. 2012a; Riccio et al. 2014). At Denali itself, higher temperature thermochronological methods ($^{40}\text{Ar}/^{39}\text{Ar}$ multi-diffusion domain (MDD) modeling) reveal an episode of more rapid cooling beginning ~ 25 Ma and perhaps a lower magnitude event starting ~ 11 Ma (Benowitz et al. 2012b). As regards the Denali AFT profile, only the strong ~ 6 Ma event is revealed in the age-elevation profile, although the end of the ~ 25 Ma event may be revealed at ~ 20 Ma in the HeFTy model for sample D-39 from 5956 m (Fig. 9.6d). The possible ~ 11 Ma event is not significant enough to be revealed in the AFT age profile or within HeFTy models. However, this episode may contribute to the estimated pre-late Miocene cooling rate of $2\text{--}3$ $^{\circ}\text{C}/\text{Myr}$.

As new thermochronologic data are obtained from the Denali massif and the Alaska Range, more details about the temporal and spatial patterns of cooling and exhumation will be revealed. There are outstanding questions relating to the influence of various tectonic events, the stability of the McKinley restraining bend (Buckett et al. 2016) as well as the relative roles of terrane rheology and pre-existing structures versus fault geometry and partition of strain along the Denali Fault. The Denali AFT age-elevation profile provides a firm foundation for such studies.

9.4.2 Transantarctic Mountains: First Well-Defined Example of an Exhumed PAZ

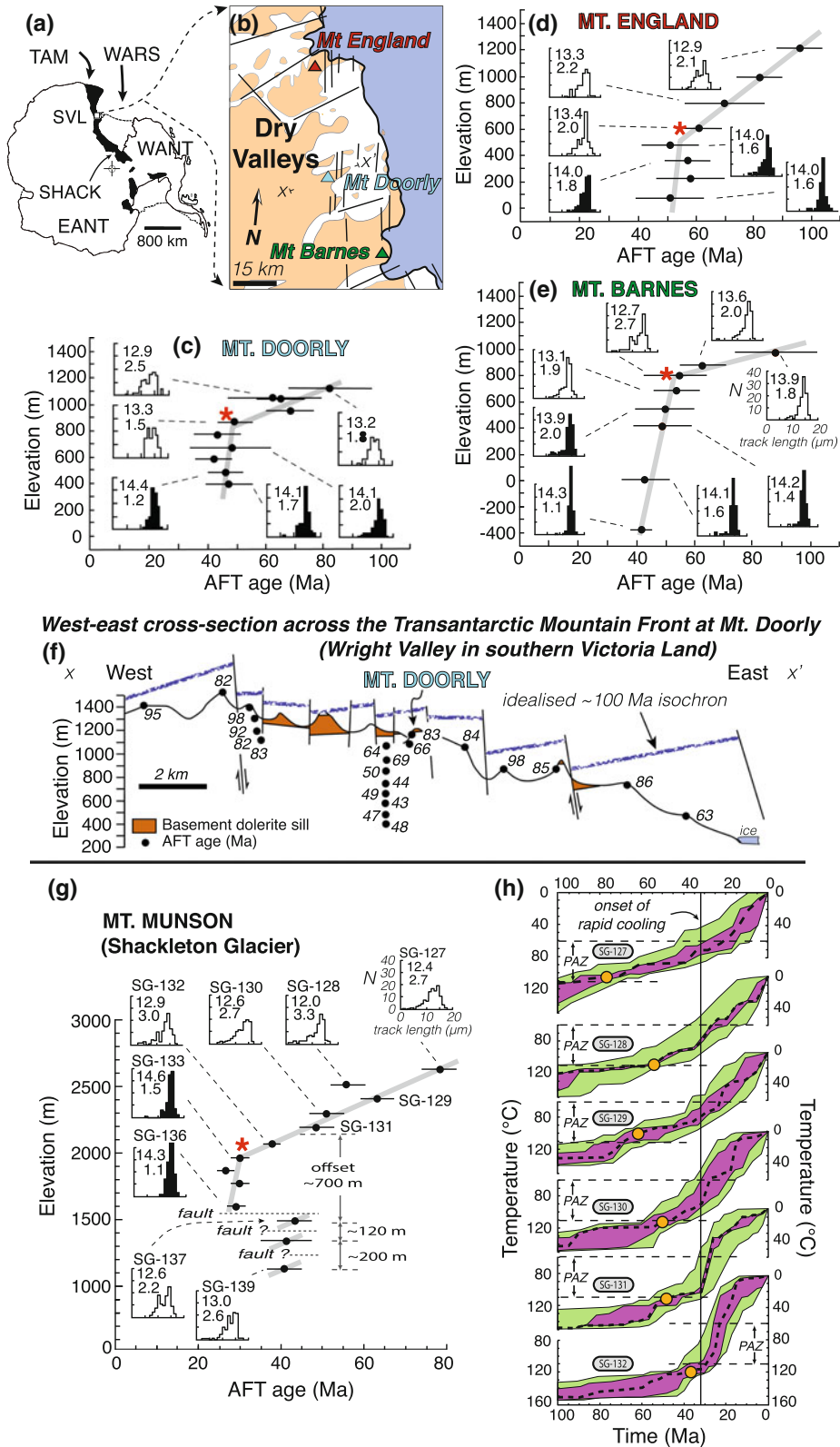
The Transantarctic Mountains (TAM), stretching ~ 3000 km across Antarctica, are the world's longest non-contractional continental mountain range. The TAM formed along a fundamental lithospheric boundary between East and West Antarctica (e.g., Dalziel 1992). In the Ross Sea sector of Antarctica, the West Antarctic rift system lies on one side and cratonic East Antarctica on the other (Fig. 9.7a). The TAM reach elevations as high as ~ 4500 m and are typically $100\text{--}200$ km wide. They can be envisaged as a number of asymmetric fault blocks dipping beneath the East Antarctic Ice Sheet, separated by transverse structures including transfer faults or accommodation zones. Outlet glaciers, typically large and draining the East Antarctic Ice Sheet, usually occupy these transverse structures.

The Dry Valleys region of southern Victoria (Fig. 9.7b) is permanently ice-free, exposing km-scale crustal sections in the valley walls. The TAM are faulted along their boundary with the West Antarctic rift system, where faults step-down $\sim 2\text{--}5$ km across the TAM Front (e.g., Barrett 1979; Fitzgerald 1992, 2002; Miller et al. 2010). Overall, the geology of the TAM appears relatively simple. This is because of the shallow inland-dipping nature of the range defined by Devonian-Triassic Beacon Supergroup strata and thick dolerite sills and basaltic volcanics of the Ferrar Dolerite and Kirkpatrick Basalt (the Ferrar large igneous province) intruded and extruded at ~ 180 Ma (e.g., Heilmann et al. 1994). Unconformably, beneath these sedimentary and magmatic rocks are upper Proterozoic-Cambrian metamorphic rocks and Cambrian-Ordovician granites of the Granite Harbour Intrusives (e.g., Goodge 2007).

The TAM AFT data was instrumental in establishing the concept of an exhumed PAZ, notably the AFT age—elevation profile from Mt. Doorly in the Dry Valleys region (Fig. 9.7b, c) (Gleadow and Fitzgerald 1987). A ~ 800 m profile yielded AFT ages from ~ 83 to ~ 43 Ma. There is a

Fig. 9.7 **a, b** Map of Antarctica and part of the Dry Valleys area of southern Victoria Land indicating ice-free areas and faults (thin black lines), as well as location of the three vertical sampling profiles from this region. TAM = Transantarctic Mountains (black), WARS = West Antarctic rift system, SVL = southern Victoria Land, SHACK = Shackleton Glacier, WANT = West Antarctica, EANT = East Antarctica. **c–e** AFT age ($\pm 2\sigma$) versus elevation plots for Mt. Doorly, Mt. England and Mt. Barnes. The red asterisks mark the location of the break in slope indicative of the base of an exhumed PAZ and the onset of rapid cooling/exhumation. CTLDs are normalized to 100. **f** Cross section ($x\text{--}x'$ —position shown in b) along the Mt. Doorly ridge (modified from Fitzgerald 1992) showing offset dolerite sills and idealized ~ 100 Ma AFT isochron delineating the structure across this

part of the TAM Front. **g–h** AFT age ($\pm 2\sigma$) versus elevation plot for Mt. Munson in the Shackleton Glacier region, showing the onset of rapid cooling/exhumation at ~ 32 Ma and the offset of AFT ages due to faulting across the TAM Front. HeFTy inverse thermal models shown for selected samples from above the break in slope at Mt. Munson. Yellow dots = AFT ages. Models just above the break clearly show the onset of rapid cooling at ~ 32 Ma but this signal is lost only ~ 300 m above the break because the proportion of longer (rapidly cooled) to shorter (tracks residence for long periods of time in the PAZ) changes and hence for these higher elevation samples, the modeling simply indicates slow cooling since the AFT age of the sample. Figures are summarized from Gleadow and Fitzgerald (1987), Fitzgerald (1992, 2002) and Miller et al. (2010)



pronounced break in slope at an elevation of ~ 800 m, corresponding to an AFT age of ~ 50 Ma (Fig. 9.7c). CTLDs above the break in slope have the now-familiar shorter means (~ 13 μm) with broader distributions reflected in larger standard deviations near ~ 2 μm , with distributions often being bimodal. Below the break in slope, CTLDs have means >14 μm with narrow distributions reflected in their standard deviations, although there are once again still a few short tracks. Gleadow and Fitzgerald (1987) interpreted the break in slope as the base of a “fossil PAZ” that had been uplifted and preserved at higher elevations in the TAM, with uplift starting from ~ 50 Ma. Samples above the break resided in the PAZ prior to ~ 50 Ma, whereas samples below the break had an essentially zero age prior to the onset of uplift.

The Mt. Doorly age-elevation profile conclusively established the concept of an exhumed PAZ. This was due to a number of reasons:

- Gleadow and Fitzgerald (1987) renamed the “partial stability zone” as the PAZ, to denote what this pattern of ages and CTLDs represented, especially when compared to drill hole data where age and length patterns were similar (e.g., Naeser 1981; Gleadow and Duddy 1981; Gleadow et al. 1983).
- The rate of exhumation in the TAM is very slow, and the valley walls are glacially sculpted and therefore steep, so a vertical profile over only ~ 800 m relief yielded a well-defined example of an exhumed PAZ.
- The Mt. Doorly profile had a greater concentration of samples (collected every ~ 100 m of elevation), and this study was just underway when CTLDs were just starting to be routinely measured. So, while the variation of age with elevation is important and inflection points had been identified as paleoisotherms representing the base of a PAZ (Naeser 1976), age variation in conjunction with CTLDs made the interpretation of this age-elevation data more conclusive.
- The TAM study was in progress as the first thermal modeling programs—initially forward modeling, followed by inverse thermal modeling—were being developed. This allowed forward models to replicate the age-elevation trends and also the CTLDs. Interestingly, the interpretation of these data sets in the first papers was so obvious that these models were not presented, although various models started to be published in the early 1990s (e.g., Fitzgerald and Gleadow 1990; Fitzgerald 1992).

An important factor concerning interpretation and understanding of AFT data in the Dry Valleys region is the remarkable layer cake stratigraphy. Basement rocks are unconformably overlain by 2–3 km of sediments, both of which were then intruded in the Jurassic by thick (up to

300 m) sills and capped by basaltic lavas. Jurassic magmatism raised the geothermal gradient and completely reset fission-tracks during that time period for the Dry Valleys (Gleadow et al. 1984). However, some samples well inland in other parts of the TAM have been partially or not thermally reset by this Jurassic magmatism (e.g., Fitzgerald 1994; see also Chap. 13, Baldwin et al. 2018).

The level of erosion along the TAM Front is such that AFT has proven to be the best method to record the exhumation history of the TAM. The simple fault-block structure of the range usually means that the AFT results are predictable and reproducible. We demonstrate this by including two other vertical profiles from the Dry Valleys region. The Mt. England (Fitzgerald 1992) and Mt. Barnes (Fitzgerald 2002) age-elevation profiles (Fig. 9.7d, e) are remarkably similar in form and age range with Mt. Doorly. All three profiles have similar CTLDs above and below the break in slope, with similar timing of the break in slope at 50–55 Ma, and with the same interpretation. The amount of exhumation and the average rates can be calculated using a variety of approaches: the depth to T_c from measured present-day geothermal gradients or assuming a typical “stable continental” paleogeothermal gradient, reconstruction of the stratigraphy above the break in slope, the AFT “stratigraphy” approach of Brown (1991) and the slope of the age-elevation profile below the break. The amount of exhumation since the early Cenozoic is on the order of ~ 4.5 km near the edge of the TAM Front, at an average rate of ~ 100 m/Myr.

The gentle slope of the age-elevation profile above the break, largely a relict of the shape of the PAZ formed prior to ~ 50 Ma defining the AFT stratigraphy (see Sect. 9.3.2, also Chap. 10, Malusà and Fitzgerald 2018b; Chap. 11, Foster 2018; Chap. 13, Baldwin et al. 2018), can be used to constrain the location and offset of faults. This concept, well established now, but in its infancy then, was tested along the Mt. Doorly ridge (Fig. 9.7f) where offset dolerite sills are clearly visible and easily mapped, with vertical offsets well constrained (Gleadow and Fitzgerald 1987; Fitzgerald 1992). The slope of the upper part of the Doorly profile, the exhumed PAZ, is only ~ 15 m/Myr so the variation of AFT age is significant for small elevation changes, well-suited to detect fault offsets. Reconstruction of the ~ 100 Ma isochron, across mapped and unmapped faults, provides offset estimates on the displacements down to ~ 200 m, taking into account uncertainties on AFT ages and variable dip of the faulted sill segments (Fig. 9.7f).

Other age-elevation profiles throughout the Dry Valleys also reveal exhumed PAZs. These profiles may have either only the gentle upper slope or the steeper lower part, dependent on their location across the TAM. Samples collected in isolation usually have ages and CTLDs that allows them to be placed in the context of the exhumed PAZ profile revealed in these three examples. However, the age pattern

does become more complicated inland from the TAM Front because of earlier episodes of exhumation preserved in the AFT data set. Such patterns are revealed in profiles along the Ferrar Glacier west of Mt Barnes (Fitzgerald et al. 2006) and in other places along the TAM (see summary by Fitzgerald 2002 and also in Chap. 13, Baldwin et al. 2018). In some locations such as the Scott Glacier, there are multiple exhumed PAZs revealed in profiles across the mountains, which record episodic exhumation beginning in the Early Cretaceous, Late Cretaceous, and Early Cenozoic (Stump and Fitzgerald 1992; Fitzgerald and Stump 1997). Obviously, many factors including faulting, the orientation of the sampling profile with respect to structures, the steepness of the profile versus topographic effects and the possible variable effect of annealing during Jurassic magmatism may obfuscate the record.

We include in this section one more example of an exhumed PAZ from Mt. Munson (Fig. 9.7g), in the Shackleton Glacier region (Miller et al. 2010). This profile was collected starting just under the unconformity between the basement granites and the overlying Beacon Supergroup (see Chap. 13, Baldwin et al. 2018), and then down a ridge oriented across the grain of the orogen. Several small saddles along that ridge contain crush zones marking the locations of probable brittle faults. The age-elevation relationship reveals the classic form of an exhumed PAZ with CTLDs as discussed above, and a break in slope at ~ 32 Ma. This break in slope is younger than those in the Dry Valleys, for two reasons (Fitzgerald 2002). The onset of rapid cooling marked by the break in slope becomes younger along the TAM, in a general southerly direction, from ~ 55 to ~ 40 Ma. Also, observed in several locations along the TAM, there is a coast-to-inland younging trend as a result of escarpment retreat (cf., Chap. 20, Wildman et al. 2018). Near the coast, the onset of rapid cooling is ~ 40 Ma, decreasing to ~ 32 Ma at Mt. Munson about 50 km inland. Faulting (downthrown toward the coast) is evident in the Mt. Munson age-elevation plot—as revealed by three samples with older AFT ages at lower elevations (<1500 m). These

lower-elevation older samples have ages and CTLDs similar to those found at elevations above the break in slope (>2000 m), where ages are >32 Ma.

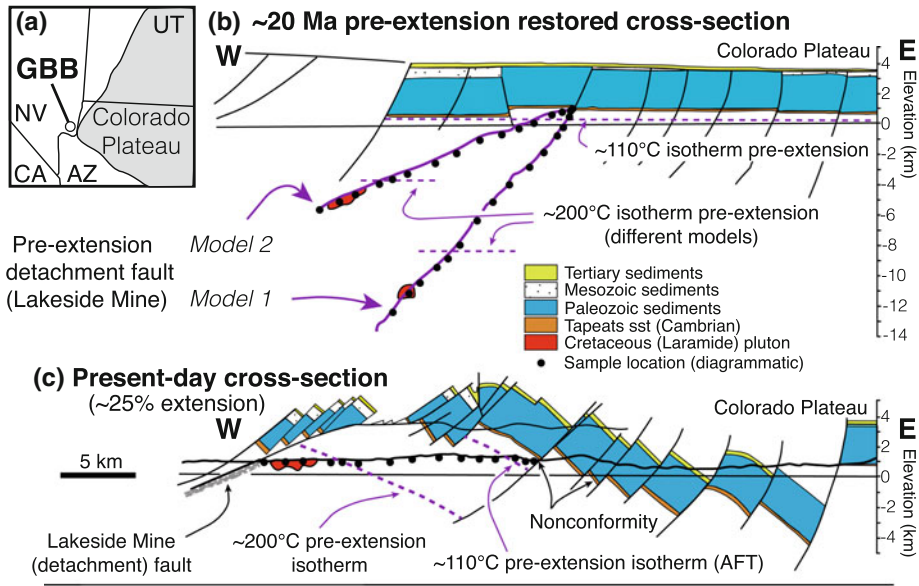
HeFTy inverse thermal models of the Mt. Munson profile (Fig. 9.7g) confirm the interpretation of an exhumed PAZ. But the main reason to present these is to show that in the models, the transition from long-term residence within the AFT PAZ (which could also be termed as slow cooling through the PAZ) prior to the onset of rapid cooling is only seen in samples lying just above the break in slope (e.g., SG-132). In samples only ~ 300 m above the break (e.g., SG-130), the rapid cooling signal is not observed, but rather the models show monotonic cooling at an averaged rate. The lack of an observed rapid cooling signal beginning ~ 32 Ma in these higher elevation/older samples results from the changing proportions of confined tracks in the distributions. In samples just above the break in slope, there is a much greater proportion of long tracks formed after ~ 32 Ma, in comparison to tracks shortened while resident in the PAZ, so the model is able to constrain the onset of rapid cooling. In contrast, for samples ~ 300 m higher in elevation above the break, AFT ages are already ~ 60 Ma. In these samples, there is in essence a 50/50 split between tracks that underwent annealing for ~ 30 Myr in the PAZ and those that record rapid cooling beginning ~ 32 Ma, and modeling does not reveal the episodic cooling.

9.4.3 Gold Butte Block: Multiple Exhumed PAZs/PRZs

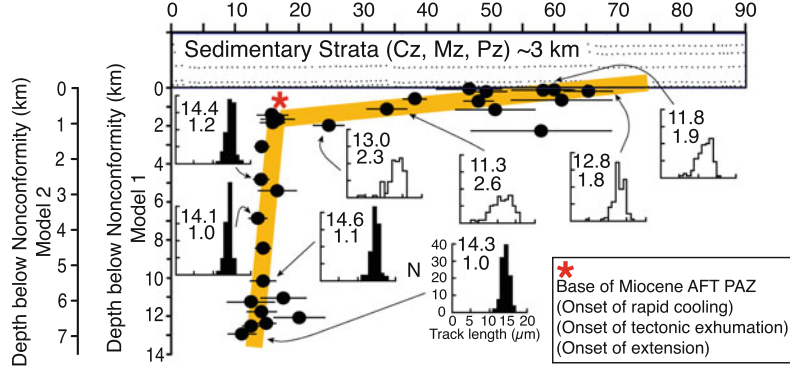
The Gold Butte Block (GBB) in southeastern Nevada lies within the eastern Lake Mead extensional domain, a zone of extension west of the Grand Canyon, Colorado Plateau, and east of the main part of the extended Basin and Range province (Fig. 9.8a–c). Bounding the west side of the GBB is the Lakeside Mine Fault, which forms the northern part of the ~ 60 km long north–south striking South Virgin–White Hills detachment fault (e.g., Duebendorfer and Sharp 1998).

Fig. 9.8 **a** Location map for the Gold Butte Block (GBB) in southeastern Nevada. **b–c** Pre-extension (~ 20 Ma) restored cross section of the GBB and present-day cross section showing two models for the pre-extension geometry of the Lakeside Mine detachment fault. Model 1 is after Wernicke and Axen (1988) and Fryxell et al. (1992), and model 2 is from Karlstrom et al. (2010). Figure modified from Karlstrom et al. (2010), their Fig. 2. The ~ 110 °C paleoisotherm is based on the restored location for the base of the restored AFT PAZ, and the ~ 200 °C isotherm (in **b**, **c** and **e**) is based on K-feldspar MDD model results as outlined in Karlstrom et al. (2010). **d** AFT data plotted versus depth below the non-conformity between basement rocks and the Cambrian Tapeats Sandstone for models 1 and 2 of the pre-extension location of the Lakeside Mine detachment fault. This figure is modified from Fitzgerald et al. (2009), but with paleodepths (for model 1 which was used in their 2009 paper) slightly recalculated according to Karlstrom et al. (2010),

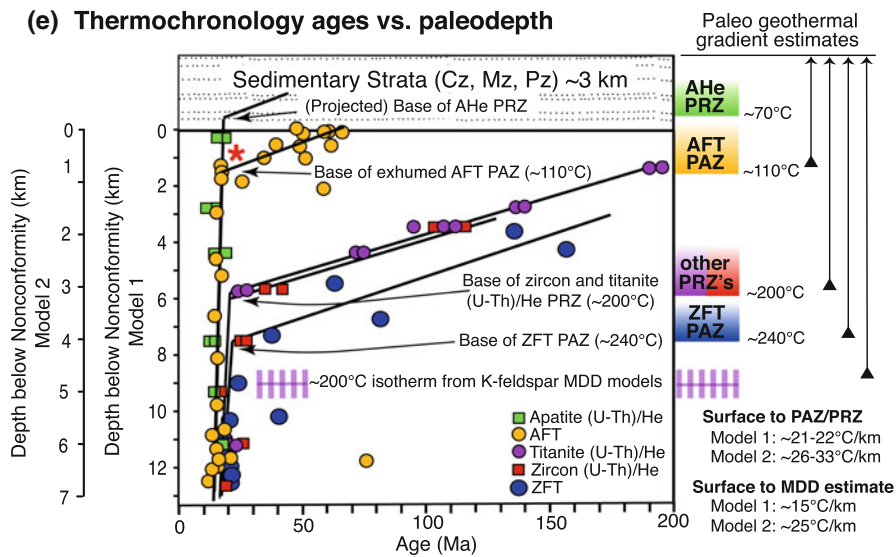
their Fig. 2, and paleodepths for model 2 from that same figure. The age-paleodepth relationship clearly shows an exhumed PAZ, with characteristic CTLDs above and below the break in slope which marks the onset of rapid cooling due to tectonic exhumation as a result of extension beginning ~ 17 Ma. **e** Age for different thermochronometers (AFT, ZFT, apatite, zircon and titanite (U–Th)/He—see text for references) plotted against paleodepths for model 1 and model 2. Uncertainties on ages are not included—to retain clarity for this figure. All methods, within error, constrain approximately the same age for the location of the base of the exhumed PAZs and PRZs, indicative of the onset of rapid cooling at ~ 17 Ma. Paleodepths were slightly recalculated as described for (d). Paleogeothermal gradients are listed for each of the models, but only for the surface to the base of each PAZ/PRZ. Paleodepth estimation is fundamental to these paleogeothermal estimates, as discussed in the text



(d) AFT data vs. paleodepth



(e) Thermochronology ages vs. paleodepth



The GBB has been described as a tilted crustal section exposing ~ 17 km of crust (Wernicke and Axen 1988; Fryxell et al. 1992; Brady et al. 2000) and as such has provided an ideal crustal section to which an almost complete suite of thermochronologic methods have been applied. The results from the various thermochronologic methods agree remarkably well, but there are some complications related to the determination of the paleodepth of samples. Estimates of the pre-extension paleogeothermal gradient are therefore also complicated, which we will also discuss briefly below.

One of the reasons the GBB is of such interest is because it was a key location for understanding the extensional structure of the crust (e.g., Wernicke and Axen 1988). During extension, the footwall of normal faults underwent isostatic uplift, the degree of which is important for evaluating contrasting models for the dip of normal faults during extension. The GBB was thought to represent an intact tilted crustal section with its western end exposing largely Proterozoic basement (paragneiss, orthogneiss, amphibolite, and various granitoids) from middle crustal levels. On its eastern side, the $\sim 50^\circ$ easterly dipping Cambrian Tapeats Sandstone, the basal unit of the famous Grand Canyon stratigraphic section, unconformably overlies basement rocks. However, more recent structural reconstructions (Karlstrom et al. 2010) indicate that this titled crustal block model may be too simple. Their new model incorporates slip on initially subhorizontal detachment faults, such that the initial depths of the deepest footwall rocks under the Lakeside Mine Detachment are much shallower. Compared to the previous estimate of ~ 17 km depth for the tilted crustal block model (shown as model 1 in Fig. 9.8), Karlstrom et al. (2010) proposed the pre-extension detachment extended to depths of ~ 10 km (model 2). We plot in Fig. 9.8b the paleodepth of all samples, for model 1 (steeper initial dip of the detachment fault) and model 2 (shallower initial dip) according to the ~ 20 Ma pre-extension structural reconstruction shown in Fig. 2 of Karlstrom et al. (2010).

AFT was the first thermochronologic method applied across the GBB. Samples were collected in basement rocks starting just below the unconformity and then west across the GBB and projected onto a line approximately parallel to the extension direction (Fitzgerald et al. 1991, 2009). The variation of AFT ages and CTLDs plotted versus paleodepth (Fig. 9.8d) reveals the classic form of an exhumed PAZ. The break in slope, middle Miocene in age (~ 15 – 17 Ma) occurs ~ 1.4 km below the unconformity indicating the onset of rapid cooling due to tectonic exhumation accompanying extension. Samples above the break were resident within or cooled slowly through the AFT PAZ. Thus, mean lengths are shorter (~ 11 – 13 μm), distributions tend toward bimodality, and standard deviations are larger (~ 2 μm or greater). In contrast, CTLDs below the break have longer means (>14 μm), unimodal distributions with smaller standard

deviations (~ 1 μm) indicative of rapid cooling. Reiners et al. (2000) subsequently applied AHe dating across the GBB. No break in slope in the AHe ages was observed in samples collected from the basement (Fig. 9.8e), but a break would likely be expected within the overlying sedimentary strata. Reiners et al. (2000, 2002) did however observe inflection points in the zircon and titanite (U–Th)/He ages, interpreted as the base of exhumed PRZs. Reiners et al. (2000, 2002) used the reconstructed paleogeothermal gradient (~ 20 $^\circ\text{C}/\text{km}$) to constrain the T_c of these two systems, as did Bernet (2009) for zircon FT (ZFT) dating. The ZFT age-paleodepth pattern represented an exhumed zircon PAZ, with samples cooling slowly before rapid cooling began in the Miocene. Bernet (2009) also combined all the existing thermochronology data, noting a common breakpoint at ~ 17 Ma, possibly slightly earlier (~ 20 Ma) for the higher temperature methods, although this is probably statistically indistinguishable. Geologic studies in the region indicate that extension lasted from ~ 17 to ~ 14 Ma (Beard 1996; Brady et al. 2000; Lamb et al. 2010; Umhoefer et al. 2010). The thermochronologic constraints on the onset of extension agree well with the geologic studies, notably the sedimentary record in localised fault-bounded basins with interbedded ash layers, which offer a finer fidelity in terms of the timing of extension and tilting of strata.

Many of the thermochronologic studies described briefly for the GBB used the relationship of ages with paleodepth to constrain either: (i) the paleogeothermal gradient, using a Miocene mean-annual temperature of 10 $^\circ\text{C}$, or (ii) the temperature of the base of a particular PAZ or PRZ, based on the estimate of paleogeothermal gradient and paleodepth of the break in slope. Thus, the location of a particular sample across the block and its paleodepth, depending on which structural model is used, is important. Outcrop exposures of the upper eastern end of the tilted section are quite complex, being offset in an en-echelon fashion. Mapped faults in the sedimentary section are also more easily identified than their possible extension into the underlying basement rocks. The determination of the map distance from the non-conformity to the sample and hence estimation of a pre-extension paleodepth slightly varies for each of the studies mentioned above, as explained by the authors in each case. Note that this middle Miocene paleogeothermal gradient was prior to the onset of extension and tectonic exhumation and erosion. During active tectonism, there would have been advection and a dynamic paleogeothermal gradient. In Fig. 9.8e, we plot the age (for the variety of techniques discussed) versus depth of each sample below the non-conformity. In essence, we have modified Fig. 3c from Fitzgerald et al. (2009), but recalculated the paleodepths according to Fig. 2 of Karlstrom et al. (2010). We use ~ 3 km for the thickness of the pre-extension sedimentary section above the non-conformity. Model 1, with its steeper initial dip, yields paleogeothermal gradients of 21 – 23 $^\circ\text{C}/\text{km}$,

from the surface to the base of the various PAZs/PRZs, whereas model 2 with its shallower initial dip yields $\sim 26\text{--}33$ °C/km. There is a greater disparity between the two models for the higher temperature methods, not only because of the varying model 1 versus model 2 paleodepths, but because of the greater uncertainty in sample location beneath the non-conformity. The estimates further diverge if the estimated ~ 200 °C paleoisotherm constrained by MDD modeling of K-feldspar $^{40}\text{Ar}/^{39}\text{Ar}$ data is used (Karlstrom et al. 2010). The MDD data is complex but constrains a continuous temperature–time path of each sample between ~ 250 and ~ 175 °C. As discussed extensively in Karlstrom et al. (2010), there is a discrepancy between the location of the ~ 200 °C isotherm constrained by these MDD modeling results and some of the other methods. Overall however the general age trends agree well. Some outlier older ages (i.e., those ages that are greater than ~ 20 Ma and which lie structurally below the base of their respective PAZ/PRZs) across the GBB, such as a ~ 77 Ma AFT age at the western (deeper) end (Fitzgerald et al. 1991) or some older ZFT ages to the west (Bernet 2009), plus 20–25 Ma zircon and titanite (U–Th)/He ages in the central part of the GBB, attest to structural complexity and possible incorporation of higher structural units within the fault zone while extension was ongoing.

The density of thermochronologic data across the GBB from a variety of different techniques, and we have not mentioned additional muscovite, biotite and hornblende $^{40}\text{Ar}/^{39}\text{Ar}$ data (Reiners et al. 2000; Karlstrom et al. 2010), or a more recent MDD K-feldspar study (Wong et al. 2014), has proven to be a great benchmark for the comparison and calibration of these different techniques. Notwithstanding the complications noted above, the concept of exhumed partial annealing and retention zones works well (Fig. 9.8e), notably as regards the timing for the onset of rapid cooling due to tectonic exhumation (~ 17 Ma). Structural mapping plus outlier ages indicate the GBB is not a simple east-titled crustal block exposing mid-crustal level rocks on its western side. In detail, the GBB is more structurally complex, as reflected by varying estimates for the pre-extension paleo-geothermal gradient which rely on structural models to constrain the paleodepth estimates of samples.

9.5 Summary and Conclusions

The collection of samples over significant relief and plotting age versus elevation to constrain the rates and timing of “uplift” (actually “exhumation”) was among the earliest applications of the then-fledgling low-temperature thermochronologic techniques, notably AFT dating (e.g., Wagner and Reimer 1972; Naeser 1976). This approach remains of fundamental importance in geologic and tectonic studies today, because rocks cool as they are exhumed. Thus,

samples collected over significant relief will reveal age variations, with ages generally increasing with increasing elevation. The thermal reference frame for data interpretation is dynamic and is modified by a number of factors:

- Surface topography modifies the shape of the isotherms under ridges and valleys, such that the isotherms are closer to the base of the valley than the top of the ridge. As a result, the slope of the age-elevation profile collected down the valley wall will overestimate the true exhumation rate.
- During rapid exhumation, isotherms are advected toward Earth’s surface, and as a result, the slope of an age-elevation profile will overestimate the true exhumation rate.
- Changing relief will change the slope of an age-elevation profile, such that the measured slope will overestimate the true exhumation rate. When samples are collected across an evolving long-wavelength topography, an inverse age-elevation slope may sometimes be obtained.

The best sampling strategy to minimise these effects is to collect samples over significant relief, on steep terrain, parallel to the structural grain of an orogen (where the curvature of near-surface isotherms is less), and where faults are less likely to be crossed. Also, it is advisable to collect samples close enough together so that the form of a profile or variations in age versus elevation trends is clearly revealed, for example, in the case of an exhumed PAZ or PRZ. An important component of any study, both prior to sampling and during the interpretation stage, is to be aware of the factors that may change the slope of the profile and hence influence interpretation of the data. Defining age-elevation profiles as “vertical profiles” may signal an understanding of these factors, and hence, the application of a sampling strategy takes them into account. In some studies, describing and interpreting an age-elevation relationship where an appropriate sampling strategy was not employed have led to suspect interpretations that are potentially incorrect.

A PAZ/PRZ forms during a time of relative thermal and tectonic stability. The age-elevation slope within a PAZ/PRZ is a function of the paleogeothermal gradient and the time over which the PAZ/PRZ forms. It is not uncommon for the form of a PAZ/PRZ to develop during periods of slow cooling as samples move slowly through the PAZ/PRZ. Long-term residence within, or slow cooling through a PAZ/PRZ, magnifies the age variation between grains or samples, especially in case of varying compositions for AFT thermochronology, and/or zonation patterns or size differences between grains for apatite and zircon (U–Th)/He dating.

If, following a period of relative stability that allows development of a PAZ/PRZ in the rock record, there is an episode of rapid cooling/exhumation, an exhumed PAZ/PRZ

may be revealed in an age-elevation profile. The break in slope (or inflection point) marks the base of the exhumed PAZ/PRZ, in effect a paleoisotherm. The timing of the break in slope marks the onset of the episode of rapid cooling/exhumation, although it is likely a slight underestimate. For AFT thermochronology, there is a distinctive pattern of CTLDs above and below the break in slope. Those above the break are broader and typically have shorter means (<13 μm), larger standard deviations (~ 2 μm or greater) and are often bimodal with a systematic pattern of varying components of shorter versus longer tracks. CTLDs below the break are typically unimodal, have longer means (>14 μm) and smaller standard deviations (<1.5 μm).

We have illustrated three examples where age-elevation profiles have proven useful in developing and testing the concept of exhumed PAZ/PRZs and have shed light on the geologic and tectonic evolution of the study regions:

- In the classic Denali example, a vertical AFT age profile collected over ~ 4 km relief reveals an exhumed PAZ, with a break in slope at ~ 6 Ma and characteristic CTLDs above and below the break. The interpretation of data from this age-elevation profile is straightforward, and geomorphic and sedimentological constraints allow the pre-uplift mean land-surface elevation to be estimated, thus allowing rock uplift, surface uplift, and exhumation to be constrained at Denali and then extrapolated to the entire central Alaska Range.
- Age-elevation profiles for AFT data collected in the Dry Valleys region of the TAM were the first to clearly reveal an exhumed PAZ, notably with the assistance of CTLDs from above and below the break in slope. The steep glaciated terrain, the overall simple and well-exposed geology, the slow exhumation rate for samples below the break, density of samples plus multiple age-elevation profiles from a relatively small region, clearly established the concept and value of the exhumed PAZ approach. The significant age variation with elevation change for samples above the break in slope, tested against down-faulted dolerite sills along the Mt. Doorly ridge system, validated the concept of using AFT stratigraphy to constrain the relatively simple fault-block structure. Using one example from Mt. Munson in the Shackleton Glacier region, we show the applicability and reproducibility of the exhumed PAZ approach along the TAM, that in places reveals episodic exhumation with preservation of multiple exhumed PAZs separated by periods of relative thermal and tectonic stability.
- In the GBB of southeastern Nevada, ages from multiple techniques (AFT, ZFT, and (U–Th)/He on apatite, zircon and titanite) plotted versus pre-extension paleodepth in the footwall of a major detachment fault reveal exhumed PAZs and PRZs that mark the onset of rapid cooling due

to tectonic exhumation at ~ 17 Ma. These data were either used to constrain pre-extension paleogeothermal gradients or alternatively constrain the temperature of the base of a particular PAZ/PRZ.

Acknowledgements PGF acknowledges research support from the Antarctic Research Centre of Victoria University of Wellington, the University of Melbourne, Syracuse University, and the National Science Foundation (Alaska, Antarctica and Gold Butte projects). PGF also thanks J. Pettinga and the Erksine Program at the University of Canterbury. Insightful and thorough reviews by Andrew Gleadow and Suzanne Baldwin and comments on various sections by Jeff Benowitz, Chilisa Shorten, and Thomas Warfel greatly improved this chapter.

References

- Abbott LD, Silver EA, Anderson RS, Smith R, Ingle JC, Kling SA, Haig D, Small E, Galewsky J, Sliter W (1997) Measurement of tectonic surface uplift rate in a young collisional mountain belt. *Nature* 385:501–508
- Baldwin SL, Lister GS (1998) Thermochronology of the South Cyclades shear zone, Ios, Greece; effects of ductile shear in the argon partial retention zone. *J Geophys Res* 103:7315–7336
- Baldwin SL, Fitzgerald PG, Malusà MG (2018) Chapter 13. Crustal exhumation of plutonic and metamorphic rocks: constraints from fission-track thermochronology. In: Malusà MG, Fitzgerald PG (eds) *Fission-track thermochronology and its application to geology*. Springer, Berlin
- Barrett PJ (1979) Proposed drilling in McMurdo Sound. *Mem Nat Inst Polar Res, Spec Issue* 13:231–239
- Batt GE, Braun J (1997) On the thermomechanical evolution of compressional orogens. *Geophys J Int* 128:364–382
- Beard LS (1996) Paleogeography of the Horse Spring Formation in relation to the Lake Mead fault system, Virgin Mountains, Nevada and Arizona. In: Bertalan KK (ed) *Reconstructing the history of Basin and Range extension using sedimentology and stratigraphy*, vol 303. Geological Society of America Special Paper, pp 27–60
- Benowitz JA, Layer PW, Armstrong PA, Perry SE, Haeussler PJ, Fitzgerald PG, Vanlaningham S (2011) Spatial variations in focused exhumation along a continental-scale strike-slip fault: the Denali fault of the eastern Alaska Range. *Geosphere* 7:455
- Benowitz JA, Haeussler PJ, Layer PW, O’Sullivan PB, Wallace WK, Gillis RJ (2012a) Cenozoic tectono-thermal history of the Tordrillo Mountains, Alaska: Paleocene-Eocene ridge subduction, decreasing relief, and late Neogene faulting. *Geochem Geophys Geosys* 13(4). <https://doi.org/10.1029/2011gc003951>
- Benowitz JA, Bemis SP, O’Sullivan PB, Layer PW, Fitzgerald PG, Perry S (2012b) The Mount McKinley Restraining Bend: Denali Fault, Alaska. *Geol Soc Am Abstr Programs* 44(7):597
- Benowitz JA, Layer PW, Vanlaningham S (2014) Persistent long-term (c. 24 Ma) exhumation in the Eastern Alaska Range constrained by stacked thermochronology. *Geol Soc Lon Spec Publ* 378:225–243
- Bernet M (2009) A field-based estimate of the zircon fission-track closure temperature. *Chem Geol* 259:181–189
- Bernet M, Garver JI (2005) Fission-track analysis of detrital zircon. *Rev Mineral Geochem* 58:205–238
- Brady RJ, Wernicke B, Fryxell JE (2000) Kinematic evolution of a large-offset continental normal fault system, South Virgin Mountains, Nevada. *Geol Soc Am Bull* 112:1375–1397
- Braun J (2002) Quantifying the effect of recent relief changes on age-elevation relationships. *Earth Planet Sci Lett* 200:331–343

- Braun J (2003) Pecube: a new finite-element code to solve the 3D heat transport equation including the effects of a time-varying, finite amplitude surface topography. *Comput Geosci* 29:787–794
- Braun J (2005) Quantitative constraints on the rate of landscape evolution derived from low-temperature thermochronology. *Rev Min Geochem* 58:351–374
- Braun J, van der Beek P, Batt G (2006) Quantitative thermochronology: numerical methods for the interpretation of thermochronological data. Cambridge University Press
- Brennan P, Gilbert H, Ridgway KD (2011) Crustal structure across the central Alaska Range: Anatomy of a Mesozoic collisional zone. *Geochem Geophys Geosyst* 12:Q04010. <https://doi.org/10.1029/2011GC003519>
- Brown R (1991) Backstacking apatite fission-track “stratigraphy”: a method for resolving the erosional and isostatic rebound components of tectonic uplift histories. *Geology* 19:74–77
- Brown RW, Summerfield MA (1997) Some uncertainties in the derivation of rates of denudation from thermochronologic data. *Earth Surf Proc Land* 22:239–248
- Brown RW, Summerfield MA, Gleadow AJW (1994) Apatite fission track analysis: its potential for the estimation of denudation rates and implications for models of long-term landscape development. In: Kirby MJ (ed) *Process models and theoretical geomorphology*. Wiley, pp 23–53
- Burkett CA, Bemis SP, Benowitz JA (2016) Along-fault migration of the Mount McKinley restraining bend of the Denali fault defined by late Quaternary fault patterns and seismicity, Denali National Park & Preserve, Alaska. *Tectonophysics* 693:489–506
- Burtner RL, Nigrini A, Donelick RA (1994) Thermochronology of Lower Cretaceous source rocks in the Idaho-Wyoming thrust belt. *AAPG Bull* 78:1613–1636
- Calk LC, Naeser CW (1973) The thermal effect of a basalt intrusion on fission tracks in quartz monzonite. *J Geol* 81:189–198
- Ching-Ying L, Typhoon L, Lee CW (1990) The Rb-Sr isotopic record in Taiwan gneisses and its tectonic implications. *Tectonophysics* 183:129–143
- Dalziel IWD (1992) Antarctica: a tale of two supercontinents. *Annu Rev Earth Planet Sci* 20:501–526
- Dodson MH (1973) Closure temperatures in cooling geochronological and petrological systems. *Contrib Mineral Petrol* 40:259–274
- Duebendorfer EM, Sharp WD (1998) Variation in extensional strain along-strike of the South Virgin-White Hills detachment fault: perspective from the northern White Hills, northwestern Arizona. *Geol Soc Am Bull* 110:1574–1589
- Dumitru TA (2000) Fission-track geochronology. In: Noller JS, Sowers JM, Lettis WR (eds) *Quaternary geochronology: methods and applications*. Wiley, Hoboken, pp 131–155
- Dusel-Bacon CE (1994) Metamorphic history of Alaska. In: Plafker G, Berg HC (eds) *The geology of North America, v G-1 The Geology of Alaska*. Geological Society of America, Boulder, CO, pp 495–533
- Ehlers TA, Farley KA (2003) Apatite (U-Th)/He thermochronometry: methods and applications to problems in tectonic and surface processes. *Earth Planet Sci Lett* 206:1–14
- England P, Molnar P (1990) Surface uplift, uplift of rocks, and exhumation of rocks. *Geology* 18:1173–1177
- Farley KA (2002) (U-Th)/He dating: techniques, calibrations, and applications. In: Porcelli D, Ballentine CJ, Wieler R (eds) *Noble gases in geochemistry and cosmochemistry*, vol 47. *Reviews Min Pet Soc Am*, pp 819–844
- Fitzgerald PG (1992) The Transantarctic Mountains of southern Victoria Land: the application of apatite fission track analysis to a rift shoulder uplift. *Tectonics* 11:634–662
- Fitzgerald PG (1994) Thermochronologic constraints on post-Paleozoic tectonic evolution of the central Transantarctic Mountains, Antarctica. *Tectonics* 13:818–836
- Fitzgerald PG (2002) Tectonics and landscape evolution of the Antarctic plate since Gondwana breakup, with an emphasis on the West Antarctic rift system and the Transantarctic Mountains. In: Gamble JA, Skinner DNB, Henrys S (eds) *Antarctica at the close of a Millennium*. Proceedings of the 8th international symposium on Antarctic Earth Science, vol 35. Royal Society of New Zealand Bulletin, pp 453–469
- Fitzgerald PG, Gleadow AJW (1988) Fission-track geochronology, tectonics and structure of the Transantarctic Mountains in northern Victoria Land, Antarctica. *Chem Geol* 73:169–198
- Fitzgerald PG, Gleadow AJW (1990) New approaches in fission track geochronology as a tectonic tool: examples from the Transantarctic Mountains. *Nucl Tracks Radiat Meas* 17:351–357
- Fitzgerald PG, Stump E (1997) Cretaceous and Cenozoic episodic denudation of the Transantarctic Mountains, Antarctica: new constraints from apatite fission track thermochronology in the Scott Glacier region. *J Geophys Res* 102:7747–7765
- Fitzgerald PG, Fryxell JE, Wernicke BP (1991) Miocene crustal extension and uplift in southeastern Nevada: constraints from apatite fission track analysis. *Geology* 19:1013–1016
- Fitzgerald PG, Stump E, Redfield TF (1993) Late Cenozoic uplift of Denali and its relation to relative plate motion and fault morphology. *Science* 259:497–499
- Fitzgerald PG, Sorkhabi RB, Redfield TF, Stump E (1995) Uplift and denudation of the central Alaska Range: a case study in the use of apatite fission-track thermochronology to determine absolute uplift parameters. *J Geophys Res* 100:20175–20191
- Fitzgerald PG, Baldwin SL, O’Sullivan PB, Webb LE (2006) Interpretation of (U-Th)/He single grain ages from slowly cooled crustal terranes: a case study from the Transantarctic Mountains of southern Victoria Land. *Chem Geol* 225:91–120
- Fitzgerald PG, Duebendorfer EM, Faulds JE, O’Sullivan PB (2009) South Virgin-White Hills detachment fault system of SE Nevada and NW Arizona: applying apatite fission track thermochronology to constrain the tectonic evolution of a major continental detachment fault. *Tectonics* 28. <https://doi.org/10.1029/2007tc002194>
- Fitzgerald PG, Roeske SM, Benowitz JA, Riccio SJ, Perry SE, Armstrong PA (2014) Alternating asymmetric topography of the Alaska Range along the strike-slip Denali Fault: strain partitioning and lithospheric control across a terrane suture zone. *Tectonics* 33. <https://doi.org/10.1002/2013tc003432>
- Fleischer RL, Price PB, Walker RM (1965) Effects of temperature, pressure, and ionization of the formation and stability of fission tracks in minerals and glasses. *J Geophys Res* 70:1497–1502
- Flowers RM, Ketcham RA, Shuster DL, Farley KA (2009) Apatite (U-Th)/He thermochronometry using a radiation damage accumulation and annealing model. *Geochim Cosmochim Acta* 73:2347–2365
- Foster DA (2018) Chapter 11. Fission-track thermochronology in structural geology and tectonic studies. In: Malusà MG, Fitzgerald PG (eds) *Fission-track thermochronology and its application to geology*. Springer, Berlin
- Fryxell JE, Salton GG, Selverstone J, Wernicke B (1992) Gold Butte crustal section, South Virgin Mountains, Nevada. *Tectonics* 11:1099–1120
- Gallagher K (2012) Transdimensional inverse thermal history modeling for quantitative thermochronology. *J Geophys Res Solid Earth* 117
- Gallagher K, Brown RW, Johnson C (1998) Fission Track Analysis and its application to geological problems. *Annu Rev Earth Planet Sci* 26:519–572
- Gallagher K, Stephenson J, Brown RW, Holmes C, Fitzgerald PG (2005) Low temperature thermochronology and modeling strategies for multiple samples 1: vertical profiles. *Earth Planet Sci Lett* 237:193–208
- Garver JJ, Brandon MT, Roden MMK, Kamp PJJ (1999) Exhumation history of orogenic highlands determined by detrital fission track thermochronology. *Geol Soc London Spec Publ* 154:283–304

- Gleadow AJW (1990) Fission track thermochronology—reconstructing the thermal and tectonic evolution of the crust. In: Pacific Rim Congress, Gold Coast, Queensland, 1990. Australasian Institute of Mining Metallurgy, pp 15–21
- Gleadow AJW, Brown RW (2000) Fission track thermochronology and the long term denudational response to tectonics. In: Summerfield MA (ed) *Geomorphology and global tectonics*. Wiley, NY, pp 57–75
- Gleadow AJW, Duddy IR (1981) A natural long term annealing experiment for apatite. *Nucl Tracks Radiat Meas* 5:169–174
- Gleadow AJW, Fitzgerald PG (1987) Uplift history and structure of the Transantarctic Mountains: new evidence from fission track dating of basement apatites in the Dry Valleys area, southern Victoria Land. *Earth Planet Sci Lett* 82:1–14
- Gleadow AJW, Duddy IR, Lovering JF (1983) Fission track analysis: a new tool for the evaluation of thermal histories and hydrocarbon potential. *APEA J* 23:93–102
- Gleadow AJW, McKelvey BC, Ferguson KU (1984) Uplift history of the Transantarctic Mountains in the Dry Valleys area, southern Victoria Land, Antarctica, from apatite fission track ages. *NZ J Geol Geophys* 27:457–464
- Gleadow AJW, Duddy IR, Green PF, Hegarty KA (1986) Fission track lengths in the apatite annealing zone and the interpretation of mixed ages. *Earth Planet Sci Lett* 78:245–254
- Goode JW (2007) Metamorphism in the Ross orogen and its bearing on Gondwana margin tectonics. *Geol Soc Am Spec Pap* 419:185–203
- Green PF, Durrani SA (1977) Annealing studies of tracks in crystals. *Nucl Tracks Radiat Meas* 1:33–39
- Green PF, Duddy IR, Gleadow AJW, Tingate PR, Laslett GM (1985) Fission-track annealing in apatite: track length measurements and the form of the Arrhenius plot. *Nucl Tracks Radiat Meas* 10:323–328
- Green P, Duddy I, Gleadow A, Tingate P, Laslett G (1986) Thermal annealing of fission tracks in apatite: 1. A qualitative description. *Chem Geol Isotope Geosci* 59:237–253
- Green P, Duddy I, Laslett G, Hegarty K, Gleadow A, Lovering J (1989) Thermal annealing of fission tracks in apatite 4. Quantitative modelling techniques and extension to geological timescales. *Chem Geol Isotope Geosci* 79:155–182
- Haeussler PJ (2008) An overview of the neotectonics of interior Alaska: far-field deformation from the Yakutat microplate collision. In: Freymueller JT, Haeussler PJ, Wesson RL, Ekström G (eds) *Active tectonics and seismic potential of Alaska*, vol 179. American Geophysical Union Monograph, pp 83–108. <https://doi.org/10.1029/179gm05>
- Haeussler PJ, O'Sullivan PB, Berger AL, Spotila JA (2008) Neogene exhumation of the Tordrillo Mountains, Alaska, and correlations with Denali (Mount McKinley). In: Freymueller JT, Haeussler PJ, Wesson RL, Ekström G (eds) *Active tectonics and seismic potential of Alaska*, vol 179. American Geophysical Union Monograph, pp 269–285. <https://doi.org/10.1029/179gm15>
- Heimann A, Fleming TH, Elliot DH, Foland KA (1994) A short interval of Jurassic continental flood basalt volcanism in Antarctica as demonstrated by $^{40}\text{Ar}/^{39}\text{Ar}$ geochronology. *Earth Planet Sci Lett* 121:19–41
- Huntington KW, Ehlers TA, Hodges KV, Whipp DM (2007) Topography, exhumation pathway, age uncertainties, and the interpretation of thermochronometer data. *Tectonics* 26
- Hurford AJ (2018) Chapter 1. An historical perspective on fission-track thermochronology. In: Malusà MG, Fitzgerald PG (eds) *Fission-track thermochronology and its application to geology*. Springer, Berlin
- Jadamec MA, Billen MI, Roeske SM (2013) Three-dimensional numerical models of flat slab subduction and the Denali fault driving deformation in south-central Alaska. *Earth Planet Sci Lett* 376:29–42
- Kamp PJJ, Tippett JM (1993) Dynamics of Pacific plate crust in the South Island (New Zealand) zone of oblique continent-continent convergence. *J Geophys Res: Solid Earth* 98:16105–16118
- Karlstrom KE, Heizler M, Quigley MC (2010) Structure and $^{40}\text{Ar}/^{39}\text{Ar}$ K-feldspar thermal history of the Gold Butte block: reevaluation of the tilted crustal section model. *Geol Soc Am Spec Pap* 463:331–352
- Ketcham RA (2005) Forward and inverse modeling of low temperature thermochronometry data. *Rev Mineral Geochem* 58:275–314
- Ketcham RA (2018) Chapter 3. Fission-track annealing: from geologic observations to thermal history modeling. In: Malusà MG, Fitzgerald PG (eds) *Fission-track thermochronology and its application to geology*. Springer, Berlin
- Ketcham R, Carter A, Donelick R, Barbarand J, Hurford A (2007) Improved modeling of fission-track annealing in apatite. *Am Mineral* 92:799–810
- Ketcham RA, Gautheron C, Tassan-Got L (2011) Accounting for long alpha-particle stopping distances in (U–Th–Sm)/He geochronology: refinement of the baseline case. *Geochim Cosmochim Acta* 75:7779–7791
- Lamb MA, Martin KL, Hickson TA, Umhoefer PJ, Eaton L (2010) Stratigraphy and age of the Lower Horse Spring Formation in the Longwell Ridges area, southern Nevada: implications for tectonic interpretations. *Geol Soc Am Spec Pap* 463:171–201
- Lock J, Willett S (2008) Low-temperature thermochronometric ages in fold-and-thrust belts. *Tectonophysics* 456:147–162
- Malusà MG, Fitzgerald PG (2018a) Chapter 8. From cooling to exhumation: setting the reference frame for the interpretation of thermochronologic data. In: Malusà MG, Fitzgerald PG (eds) *Fission-track thermochronology and its application to geology*. Springer, Berlin
- Malusà MG, Fitzgerald PG (2018b) Chapter 10. Application of thermochronology to geologic problems: bedrock and detrital approaches. In: Malusà MG, Fitzgerald PG (eds) *Fission-track thermochronology and its application to geology*. Springer, Berlin
- Mancktelow NS, Grasemann B (1997) Time-dependent effects of heat advection and topography on cooling histories during erosion. *Tectonophysics* 270:167–195
- Meesters AGCA, Dunai TJ (2002) Solving the production-diffusion equation for finite diffusion domains of various shapes (part II): application to cases with a-ejection and non-homogeneous distribution of the source. *Chem Geol* 186:347–363
- Metcalfe JR, Fitzgerald PG, Baldwin SL, Muñoz JA (2009) Thermochronology in a convergent orogen: constraints on thrust faulting and exhumation from the Maladeta Pluton in the Axial Zone of the Central Pyrenees. *Earth Planet Sci Lett* 287:488–503
- Miller SR, Fitzgerald PG, Baldwin SL (2010) Cenozoic range-front faulting and development of the Transantarctic Mountains near Cape Surprise, Antarctica: thermochronologic and geomorphologic constraints. *Tectonics* 29. <https://doi.org/10.1029/2009tc002457>
- Moore MA, England PC (2001) On the inference of denudation rates from cooling ages of minerals. *Earth Planet Sci Lett* 185:265–284
- Naeser CW (1976) Fission track dating. USGS Open-File Report, pp 76–190
- Naeser CW (1979) Thermal history of sedimentary basins: fission track dating of subsurface rocks. In: Scholle PA, Schluger PR (eds) *Aspects of diagenesis*, vol 26, Spec Pub Soc Econ Geol Paleo Min, pp 109–112
- Naeser CW (1981) The fading of fission-tracks in the geologic environment—data from deep drill holes. *Nucl Tracks Radiat Meas* 5:248–250
- Naeser C, Faul H (1969) Fission track annealing in apatite and sphene. *J Geophys Res* 74:705–710
- Parrish RR (1985) Some cautions which should be exercised when interpreting fission track and other dates with regard to uplift rate calculations. *Nucl Tracks Radiat Meas* 10:425

- Perry S (2013) Thermotectonic evolution of the Alaska Range: low-temperature thermochronologic constraints. PhD thesis, Syracuse University, 204 p
- Plafker G, Naeser CW, Zimmerman RA, Lull JS, Hudson T (1992) Cenozoic uplift history of the Mount McKinley area in the central Alaska Range based on fission track dating. *USGS Bull* 2041:202–212
- Reed BL, Nelson SW (1977) Geologic map of the Talkeetna quadrangle, Alaska. *USGS Misc. Field Studies Map* 870-A
- Reiners PW, Brandon MT (2006) Using thermochronology to understand orogenic erosion. *Annu Rev Earth Planet Sci* 34:419–466
- Reiners PW, Farley KA (2001) Influence of crystal size on apatite (U–Th)/He thermochronology: an example from the Bighorn Mountains, Wyoming. *Earth Planet Sci Lett* 188:413–420
- Reiners PW, Brady R, Farley KA, Fryxell JE, Wernicke B, Lux D (2000) Helium and argon thermochronometry of the Gold Butte Block, south Virgin Mountains, Nevada. *Earth Planet Sci Lett* 178:315–326
- Reiners PW, Farley KA, Hickes HJ (2002) He diffusion and (U–Th)/He thermochronometry of zircon: initial results from Fish Canyon Tuff and Gold Butte. *Tectonophysics* 349:297–308
- Reiners PW, Zhou Z, Ehlers TA, Changhai X, Brandon MT, Donelick RA, Nicolescu S (2003) Post-orogenic evolution of the Dabie Shan, eastern China, from (U–Th)/He and fission track thermochronology. *Am J Sci* 303:489–518
- Riccio SJ, Fitzgerald PG, Benowitz JA, Roeske SM (2014) The role of thrust faulting in the formation of the eastern Alaska Range: thermochronological constraints from the Susitna Glacier Thrust Fault region of the intracontinental strike-slip Denali Fault system. *Tectonics* 33. <https://doi.org/10.1002/2014tc003646>
- Schildgen T, van der Beek P (2018) Chapter 19. Application of low-temperature thermochronology to the geomorphology of orogenic systems. In: Malusà MG, Fitzgerald PG (eds) *Fission-track thermochronology and its application to geology*. Springer, Berlin
- Stump E, Fitzgerald PG (1992) Episodic uplift of the Transantarctic Mountains. *Geology* 20:161–164
- Stüwe K, Hintermüller M (2000) Topography and isotherms revisited: the influence of laterally migrating drainage divides. *Earth Planet Sci Lett* 184:287–303
- Stüwe K, White L, Brown R (1994) The influence of eroding topography on steady-state isotherms: application to fission track analysis. *Earth Planet Sci Lett* 124:63–74
- ter Voorde M, de Bruijne CH, Cloetingh SAPL, Andriessen PAM (2004) Thermal consequences of thrust faulting: simultaneous versus successive fault activation and exhumation. *Earth Planet Sci Lett* 223:395–413
- Trop JM, Ridgway KD (2007) Mesozoic and Cenozoic tectonic growth of southern Alaska: a sedimentary basin perspective. *Geol Soc Am Spec Pap* 431:55–94
- Umhoefer PJ, Beard LS, Martin KL, Blythe N (2010) From detachment to transtensional faulting: a model for the Lake Mead extensional domain based on new ages and correlation of subbasins. *Geol Soc Am Spec Pap* 463:371–394
- Valla PG, Herman F, van der Beek PA, Braun J (2010) Inversion of thermochronological age-elevation profiles to extract independent estimates of denudation and relief history—I: theory and conceptual model. *Earth Planet Sci Lett* 295:511–522
- van der Beek P, van Melle J, Guillot S, Pêcher A, Reiners PW, Nicolescu S, Latif M (2009) Eocene Tibetan plateau remnants preserved in the northwest Himalaya. *Nat Geosci* 2:364–368
- Veenstra E, Christensen DH, Abers GA, Ferris A (2006) Crustal thickness variation in south-central Alaska. *Geology* 34: 781–784
- Wagner GA, Reimer GM (1972) Fission track tectonics: the tectonic interpretation of fission track apatite ages. *Earth Planet Sci Lett* 14:263–268
- Wagner GA, Reimer GM, Jäger E (1977) Cooling ages derived by apatite fission-track, mica Rb–Sr and K–Ar dating: the uplift and cooling history of the Central Alps. *Mem Inst Geol Mineral Univ Padova* 30:1–27
- Ward DJ, Anderson RS, Haeussler PJ (2012) Scaling the Teflon Peaks: rock type and the generation of extreme relief in the glaciated western Alaska Range. *J Geophys Res* 117:1–20. <https://doi.org/10.1029/2011JF002068>
- Wildman M, Beucher R, Cogné N (2018) Chapter 20. Fission-track thermochronology applied to the evolution of passive continental margins. In: Malusà MG, Fitzgerald PG (eds) *Fission-track thermochronology and its application to geology*. Springer, Berlin
- Wernicke B, Axen GJ (1988) On the role of isostasy in the evolution of normal fault systems. *Geology* 16:848–861
- Wolf RA, Farley KA, Kass DM (1998) Modeling of the temperature sensitivity of the apatite (U–Th)/He thermochronometer. *Chem Geol* 148:105–114
- Wong M, Roesler D, Gans PB, Zeitler PK, Idleman BD (2014) Field calibration studies of continuous thermal histories derived from multiple diffusion domain (MDD) modeling of $^{40}\text{Ar}/^{39}\text{Ar}$ K-feldspar analyses at the Grayback and Gold Butte Normal Fault Blocks, US Basin and Range. *Am Geophys Union, Fall Meeting, abstract #EP21A-3521*